Review

Biodiesel Additives Synthesis Using Solid Heteropolyacid Catalysts

Marcio Jose da Silva * , **Neide Paloma Gonçalves Lopes and Alana Alves Rodrigues**

Chemistry Department, Federal University of Viçosa, Viçosa 36590-000, Brazil
* Correspondence: silvamj2003@ufv.br

Abstract: Fossil additives are a primary energy source and their contribution is around 80% in the world. Therefore, bioadditives that reduce their impact are each very important. This article discusses the chemical transformation of glycerol to carbonate, ethers, esters, ketals, and acetals, compounds with high technological applications, especially in the fuel sector as bioadditives. Mainly, heterogeneous catalysts are important in the production of more than 80% of chemicals in the word. The focus is on demonstrating how the Keggin heteropolyacids (HPAs) are efficient catalysts in the reactions of syntheses of glycerol-derived bioadditives, either in homogeneous or heterogeneous phases. Although solid, HPAs have a low surface area and are soluble in polar solvents, hampering their use as heterogeneous catalysts. Alternatively, they have been successfully used supported on solid matrixes with a high surface area. Another option is converting the Keggin HPAs to insoluble salts simply by exchanging their protons with large cations like potassium, cesium, or ammonium-derivatives. Therefore, solid heteropoly salts have reduced the cost and the environmental impact of bioadditive synthesis processes, being an alternative to traditional mineral acids or solid-supported catalysts. This review describes the most recent advances achieved in the processes of synthesis of glycerol-derived bioadditives over solid-supported HPAs or their solid heteropoly salts.

Keywords: Keggin heteropolyacids; heteropoly salts; solketal; glycerol ethers; glycerol carbonate; glycerol esters

1. Introduction

Biodiesel is a renewable and biodegradable origin fuel that is less pollutant than fossil diesel and can be produced from esterification or transesterification of non-edible or edible vegetal oils or animal fats [1]. Since it has similar properties to diesel, it can be blended within the range of 20% in volume without compromising the properties of diesel [2]. Despite its advantages, the production of biodiesel generates as a by-product, glycerol, at 10 wt.% [3]. This surplus of glycerol has motivated the development of processes to convert glycerol into products with higher value added [4]. Among the several glycerol-derived products, those that can be used as bioadditives have raised a lot of attention. Undeniably, to develop sustainable and clean pathways to upgrade glycerol into value-added chemicals and fuels would boost the biodiesel industry [5].

The use of glycerol crude in combustion engines is not possible due to the combustion properties (i.e., lower calorific value, higher viscosity, and/or auto-ignition temperature); therefore, it should be converted into products with more adequate properties to be used as bioadditives [6]. There is a plethora of bioadditives that can be obtained from glycerol; ethers, esters, ketals, acetals, and carbonates are the main examples [7]. These glycerol derivatives can enhance the cold-flow properties of biodiesel or diesel because they diminish their viscosity and reduce particulate emission and gum formation [8]. They may be used as anti-knock additives and octane boosters in spark-ignition (SI) engines [7]. These bioadditives may replace commercial fuel additives, such as methyl *tert*-butyl ether (MTBE) [9].

In general, these syntheses are carried out in the presence of a mineral acid catalyst under homogeneous conditions [10,11]. Nonetheless, these corrosive processes lead to

a large effluent generation in the steps of purification and product neutralization [12]. Moreover, although inexpensive, these soluble catalysts are difficult to recycle [13].

Solid acid catalysts are an attractive option because are easier to handle, are less corrosive, and allow a simple recovery and reuse [14]. Metal salts and oxides, zeolites, clays, sulfonic acid resins, and sulfonated carbon materials are only some examples of solid catalysts used in esterification, etherification, acetalization, or ketalization processes [15–19]. To obtain an effective solid catalyst it is necessary to combine a high surface area with a strong strength of acidity [20]. Nonetheless, the synthesis of a solid with a high surface area is generally a multi-step process, laborious, and needs thermal treatment steps [21]. Mesoporous molecular sieves such as MCM–41, SBA–3, and SBA–15 are only some examples [22,23]. However, materials like these supports have no Brønsted acidity strength, thus being inactive catalysts. A strategy that is usually adopted is the supporting of active dopants on these materials that have a high surface area [24]. The main challenge to be overcome for these catalysts is to resist the leaching triggered by high medium polarity and the deactivation problems [25].

Keggin heteropolyacids (HPAs) are active in several acid-catalyzed reactions when solved, due to the high strength of acidity [26]. In nature, they are solid; nonetheless, they have a very low surface area. Like other acid compounds, they have been used as solid-supported catalysts [27]. Nonetheless, as earlier mentioned, they still need special attention due to the leaching problems [28].

An alternative that has been successfully used is to convert the Keggin heteropolyacids (HPAs) into insoluble salts that have a high surface area [29]. This can be achieved by total or partial exchanging of the protons present in the HPAs with cations with an ionic radius greater than 1.30 Angstroms [30]. Cesium, potassium, and ammonium-derived cations are only some examples of solid heteropoly salt catalysts [31,32]. Keggin HPAs have been extensively used as catalysts to produce biofuel and/or bioadditives [31–33]. Esterification reactions of FFA, transesterification of vegetal oils, and conversion of glycerol to bioadditives are only some examples [33].

In this review, the focus is to describe the most recent advances reached in the HPAs-catalyzed reactions that produce bioadditives, starting from renewable glycerol. Both HPA solid-supported catalyzed processes and those carried out in the presence of solid heteropoly salts will be addressed. Esterification, etherification, carbonylation, acetalization, and ketalization of glycerol will be the reactions discussed.

2. Main Processes to Convert Glycerol into Bioadditives

2.1. Esterification Reactions of Glycerol

The inevitable depletion of fossil fuels has contributed to a rapid increase in biodiesel production, leading to a surplus of glycerol in the market. Therefore, it has become highly desirable to develop processes to convert glycerol into more valued chemicals [33]. Glycerol esters have several industrial applications (Figure 1).

Among the several processes, converting glycerol to acetates has been a valuable route to produce compounds that are useful for various industries. Mono-, di-, and tri-glyceryl acetate (i.e., MAG, DAG, and TAG, respectively), are products widely applied as antifreeze agents and are raw materials in the polyester and cosmetics industries (Scheme 1) [34].

DAG and mainly TAG esters have adequate properties to be used as bioadditives for liquid fuels because they can improve their cold viscosity and cetane number, reduce the cloud point, and diminish the emission of particulate materials and production of greenhouse effect gases [35]. Therefore, they are potential candidates to replace methyl tertbutyl ether (MTBE), an additive whose use has raised several controversies [35].

Conventionally, glycerol esterification reactions with acetic acid occur in the presence of homogeneous Brønsted acids; notwithstanding, these processes have drawbacks such as the large effluent generation, high corrosivity of the catalyst, and the necessity of neutralization steps [36]. Although soluble liquid catalysts such as HCl and H_2SO_4 are hard to recover, Keggin HPA catalysts are solid when pure. Although they are soluble in

polar solvents and used in a homogeneous phase, they can be recovered from the reaction medium after vaporization of the solvent or extraction with water, allowing cycles of recovery/reuse [37].
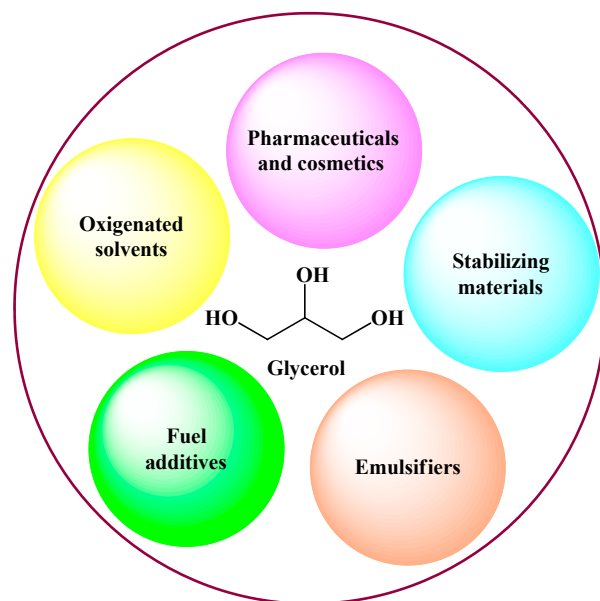

Figure 1. Industrial applications of glycerol esters (adapted from ref. [33]).
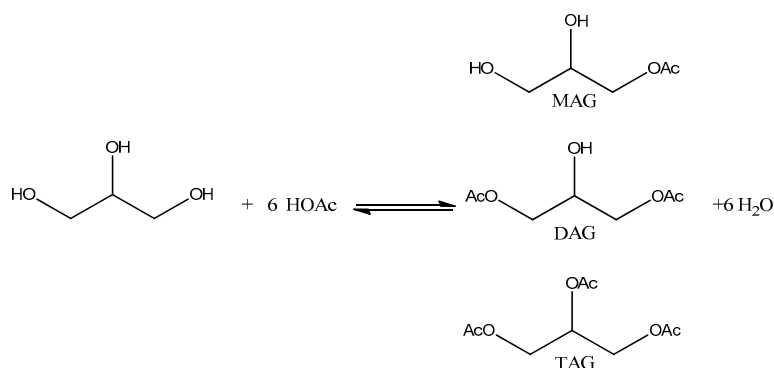
Scheme 1. Main products of glycerol acetylation with acetic acid (HOAc).

Nowadays, it has become highly desirable to develop heterogeneous acid catalysts for greener esterification processes. Various solid acid catalysts have been developed, including sulfated active carbon and metal oxides such as zeolites, alumina, zirconia, and niobium, and applied in esterification reactions of glycerol with acetic acid [38–41]. Nonetheless, in this work, we will focus only on the Keggin heteropolyacids, which are used as solid-supported catalysts or as solid salts.

2.1.1. Esterification Reactions of Glycerol over Solid-Supported HPAs

Keggin HPAs have acidity strengths approximately 1000 times higher than sulfuric acid, but are solids with low surface area and are soluble in polar solvents, aspects that add difficulty to their use as heterogeneous catalysts. Therefore, HPA catalysts have been supported on different metal oxides [41]. Although the proton exchanges with cesium make the HPAs insoluble salts, sometimes these salts are supported on solid supports such as mesoporous zirconia or silicon [42–44].

Zhu et al. synthesized a series of solid-supported HPA/ZrO$_2$ catalysts and evaluated their activity in glycerol esterification reactions with acetic acid [45]. Figure 2 shows that although their surface area was almost the same (from 49.3 to 52.5 m^2/g), the **conversions** were very different; H$_4$SiW$_{12}$O$_{40}$/ZrO$_2$ >> H$_3$PW$_{12}$O$_{40}$/ZrO$_2$, >> H$_3$PMo$_{12}$O$_{40}$/ZrO$_2$.

Conversely, the selectivity of the reactions was very close; DAG was always the main product, and MAG and TAG were the minor products formed.
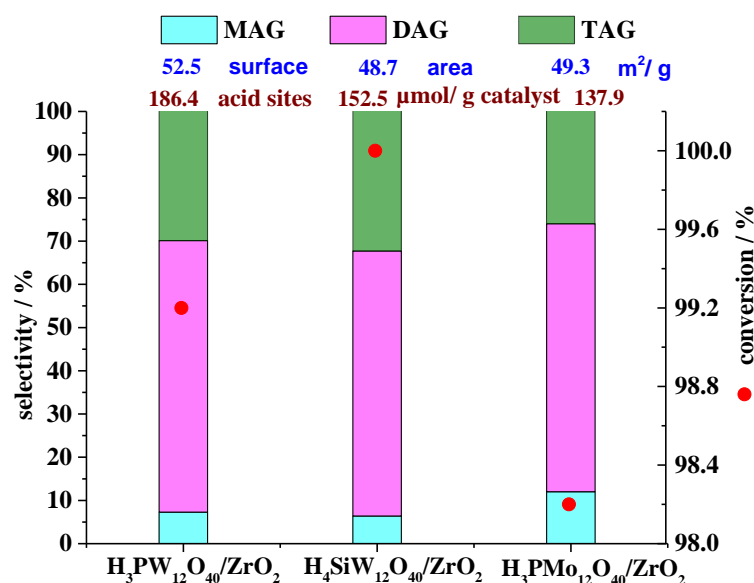

Figure 2. Catalytic performance of glycerol esterification with acetic acid over different HPA/ZrO$_2$ catalysts (adapted from ref. [45]). Reaction conditions: reaction temperature (393 K); the molar ratio of glycerol to acetic acid (1:10); catalyst amount (0.3 g).

Zhu et al. ascribed the best performance accomplished by the H$_4$SiW$_{12}$O$_{40}$/ZrO$_2$ catalyst to the exact combination of surface Brønsted acid sites and high thermal stability [45].

Lingaiah et al. prepared a series of H$_3$PW$_{12}$O$_{40}$/Nb$_2$O$_5$ catalysts which were evaluated in glycerol esterification reactions with HOAc [46]. The main effects evaluated were the catalyst load on niobium oxide and the reaction time. Figure 3 shows that, the greater the catalyst load, the higher the initial conversion, which was verified after 1 h of reaction. Phosphotungstic acid has the strongest Brønsted acidity strength; consequently, a higher load leads to a higher number of acid sites available.
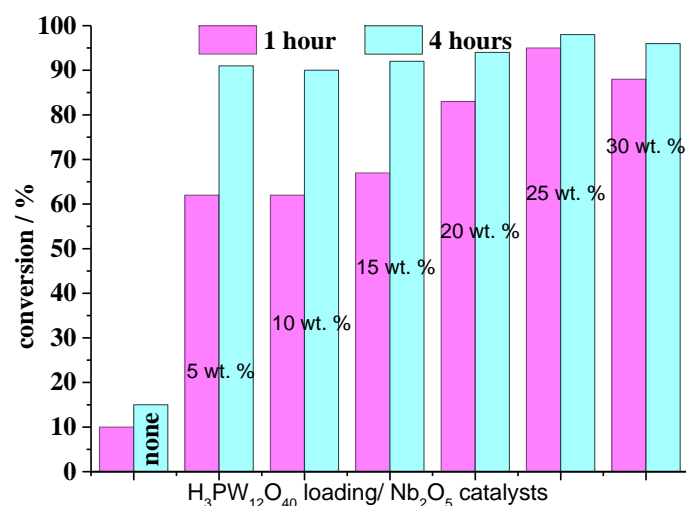

Figure 3. Impact of H$_3$PW$_{12}$O$_{40}$ load on niobium in the glycerol esterification with HOAc. Reaction conditions: reaction temperature (393 K); catalyst weight (200 mg); glycerol/acetic acid molar ratio (1:5); reaction time (1 h) (adapted from ref. [46]).

Those authors verified some important aspects in terms of selectivity; for the reaction that reached the highest conversion (25 wt.%; 95% of conversion after 1 h; Table 1, Figure 3), the selectivities to MAG and DAG were close (44 and 51%, Table 1).

Table 1. Effect of reaction time during glycerol acetylation over 25% $H_3PW_{12}O_{40}/Nb_2O_5$ catalysts.

Time/h	Glycerol Conversion/%	Selectivity/%		
		MAG	**DAG**	**TAG**
1	95	44	51	5
4	98	24	57	19

Reaction conditions: reaction temperature (393 K), catalyst weight (200 mg), glycerol to acetic acid molar ratio (1:5) (adapted from ref. [46]).

Nonetheless, after this period, MAG and DAG continued reacting with the HOAc; consequently, the selectivities toward DAG and TAG were progressively increasing, as demonstrated by the selectivity that was reached after 4 h of reaction. This is evidence of the consecutive character of these reactions (Table 1).

Castanheiro et al. prepared a series of $H_3PMo_{12}O_{40}$ encaged in the NaUSY zeolite and assessed their catalytic activity in esterification reactions of glycerol with acetic acid (Figure 4) [47]. Figure 4 shows the impact of variation of $H_3PMo_{12}O_{40}$ loading encaged in the NaUSY zeolite on the conversion and selectivity of glycerol esterification reactions. Additionally, the surface area data of various catalysts are also shown.
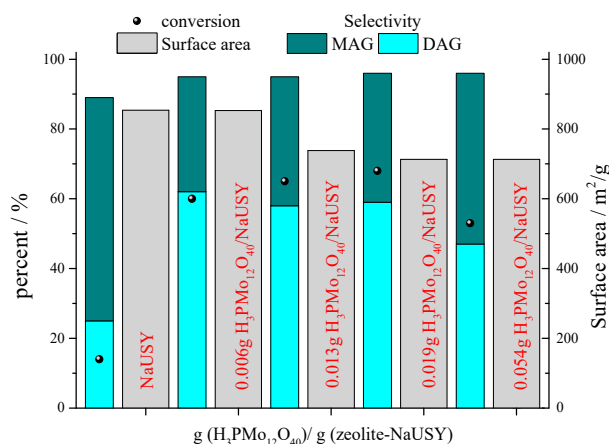
Figure 4. Surface area, conversion, and selectivity to the products of the esterification of glycerol with acetic acid over $H_3PMo_{12}O_{40}$ encaged in the NaUSY zeolite. (Adapted from ref. [47]).

The reaction conversions in Figure 3; Figure 4 were achieved under different conditions, with $H_3PWo_{12}O_{40}/Nb_2O_5$ or $H_3PMo_{12}O_{40}/NaUSY$ catalysts; however, it is possible to do a direct comparison of runs after 4 h of reaction. The last run in Figure 4 was performed with 5.4 wt.% $H_3PMo_{12}O_{40}/NaUSY$, reaching 55% conversion, while the reaction over $H_3PWo_{12}O_{40}/Nb_2O_5$ attained 93% conversion, suggesting this to be a more efficient heterogeneous catalyst.

Castanheiro et al. prepared phosphotungstic acid supported on active carbon and investigated its catalytic activity in the esterification of glycerol with acetic acid [48]. Figure 5 allows evaluation of the impact of $H_3PWo_{12}O_{40}$ loading supported on the active carbon on the conversion and reaction selectivity [48].

Noticeably, a greater catalyst load increased the glycerol conversion and favored the selectivity to DAG, although it was the main product in all the reactions. This can be attributed to the higher number of acid sites present in the support when a large catalyst load was used (Figure 5) [48].

Comparison of the conversion achieved in Figure 5 using 4.9 wt.% over $H_3PW_{12}O_{40}/AC$ with that achieved in Figure 3 ($H_3PW_{12}O_{40}/Nb_2O_5$) allows the conclusion that the acidity of the niobium support may have been the responsible factor for the superior performance of this last catalyst.
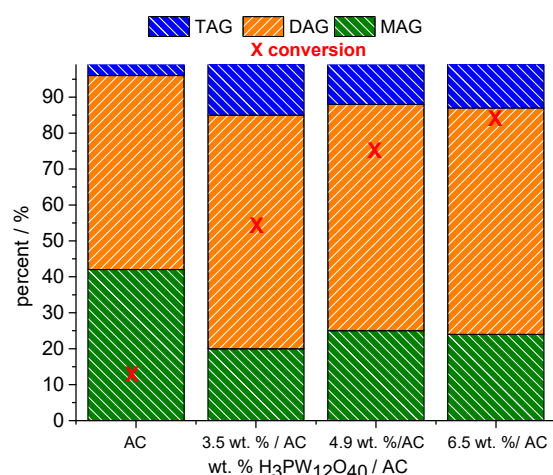
Figure 5. Conversion and selectivity to the products of the esterification of glycerol with acetic acid over $H_3PW_{12}O_{40}$/AC catalyst (adapted from ref. [48]). Reaction conditions: molar ratio of glycerol to acetic acid (1:16); temperature (393 K); catalyst loading (0.2 g).

Glycerol has been esterified with acetic acid over different solid acid catalysts. For instance, phosphotungstic, silicotungstic, and phosphomolybdic acids were prepared by impregnating or supporting different solid matrixes. Lingaiah et al. evaluated this reaction over tungstophosphoric acid supported on Cs-containing zirconia $H_3PW_{12}O_{40}$/Cs-ZrO$_2$ [49].

While in the absence of Cs, the $H_3PW_{12}O_{40}$/ZrO$_2$−catalyzed esterification of glycerol achieved 75% conversion; the addition of cesium made the conversion reach a minimum of 90% (Figure 6) [49].
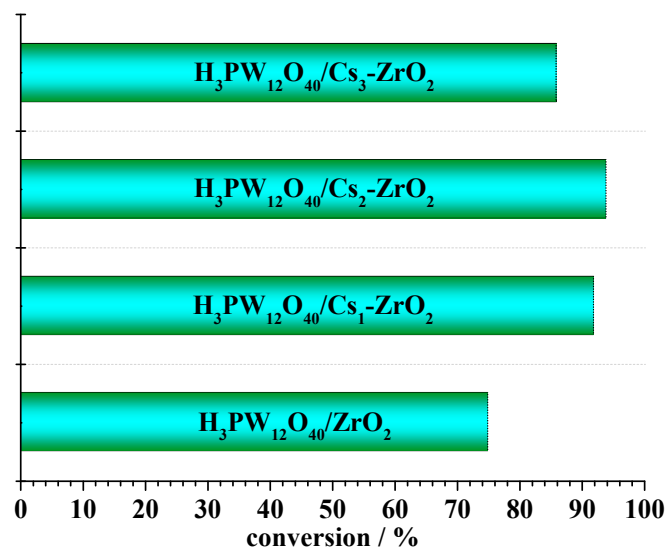

Figure 6. Esterification of glycerol with HOAc over phosphotungstic acid supported on Cs−containing ZrO$_2$ ($H_3PW_{12}O_{40}$/Cs ZrO$_2$) (adapted from ref. [49]).

Ferreira et al. immobilized the $H_3PW_{12}O_{40}$ catalyst into a silica matrix through two different techniques: the sol-gel and impregnation methods [50]. Those authors assessed the activity of these HPA catalysts in acetylation reactions of glycerol [50]. In Figure 7, the conversions achieved in esterification reactions of glycerol were correlated to the measurements of acidity strength, estimated from the values of initial electrode potential (i.e., Ei) obtained from titration curves with *n*-butylamine, the surface area obtained from adsorption-desorption isotherms by the BET method, and the catalyst loading [50].
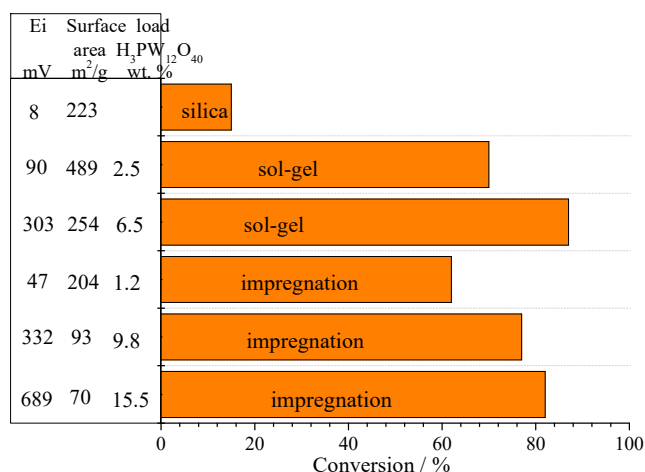
Figure 7. Effect of acidity strength, surface area, synthesis method, and $H_3PW_{12}O_{40}/SiO_2$ catalyst loading on the conversion of glycerol esterification reactions with acetic acid (adapted from ref. [50]). Reaction conditions: molar ratio of glycerol to acetic acid (1:16); temperature (393 K); catalyst (2.0 g).

Acidity and surface area are key aspects for an active heterogeneous catalyst. Indeed, the stronger acid (Ei = 689) eV attained the second highest conversion. However, it has a lower surface area. Conversely, the catalyst with the highest surface area also achieved a high conversion; however, it has a weaker acidity strength. The catalyst where these two parameters were better combined achieved the highest conversion.

The reactions carried out over the $H_3PW_{12}O_{40}/SiO_2$ catalyst prepared by the sol-gel method attained the highest conversion (Figure 8). Among the catalysts obtained from the impregnation route, those with the highest acidity strength (i.e., the highest initial electrode potential (Ei)) achieved the greatest conversion. It was possible to conclude that the surface area did not play an essential role in these reactions.
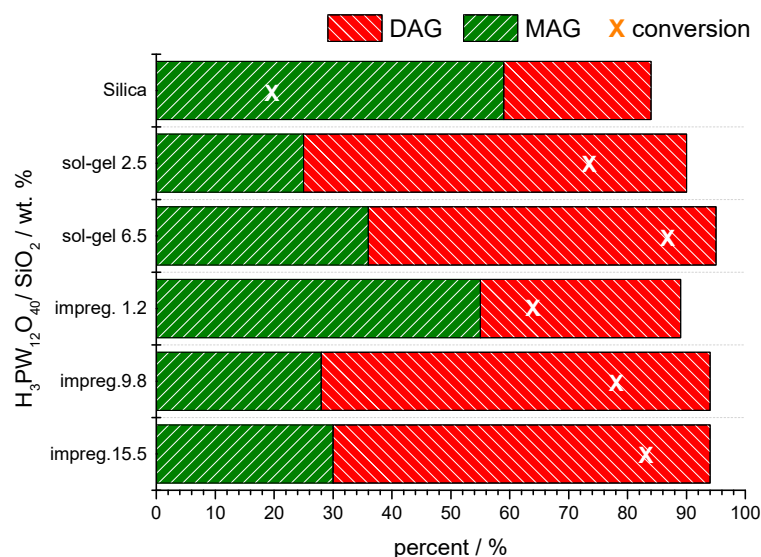

Figure 8. Impact of catalyst loading on the conversion and selectivity of the main reaction products of the esterification of glycerol with acetic acid over $H_3PW_{12}O_{40}/SiO_2$ (adapted from ref. [50]). Reaction conditions: molar ratio of glycerol to acetic acid (1:16); temperature (393 K); catalyst weight (2.0 g).

Regardless of the loading or method of synthesis, all the catalysts provided DAG as the main product, except in the reaction in the presence of the catalyst prepared through the impregnation with 1.2 wt.% [50]. This is evidence of the high efficiency of these catalysts.

Magar et al. prepared different solid acid catalysts (i.e., phosphotungstic, silico-tungstic, and phosphomolybdic acids), impregnating them on the polymeric material

polyvinylpyrrolidone [51]. The conversion and selectivity achieved in the glycerol esterification reactions with acetic acid over these polyvinyl-supported HPAs are shown in Figure 9.
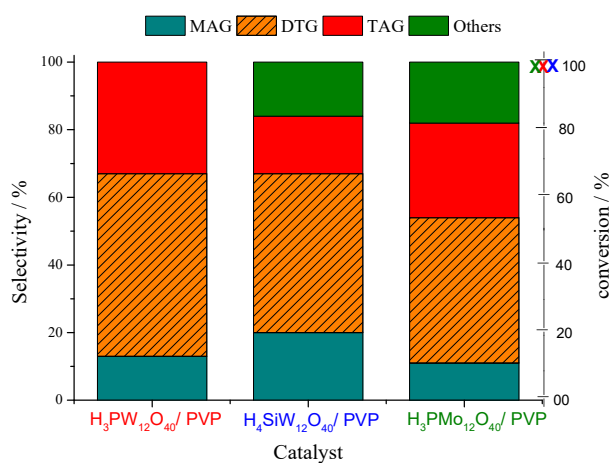

Figure 9. Glycerol esterification with acetic acid over polypyrrole polymer-supported Keggin HPAs (HPA/PVP) (adapted from ref. [51]).

Those authors verified that all the reactions carried out over the heteropolyacid-polypyrrole support accomplished an almost complete conversion [51]. Nonetheless, the $H_3PW_{12}O_{40}$/PVP-catalyzed reaction was the most selective toward the formation of the esters, because the reactions in the presence of $H_3PMo_{12}O_{40}$/PVP and $H_4SiW_{12}O_{40}$/PVP catalysts provided undesirable products. In addition, DAG, and TAG, which are the true fuel bioadditives, were more selectively obtained in the $H_3PW_{12}O_{40}$/PVP-catalyzed reaction.

Pithadia and Patel anchored silicotungstic acid on the nanoporous MCM−48 molecular sieves by the impregnation method and evaluated them in glycerol esterification with acetic acid [34].

The reaction monitoring of glycerol esterification over $H_4SiW_{12}O_{40}$/nMCM−48 catalysts showed that, while a high conversion was quickly achieved within the first hour of reaction (78%), the selectivity of products changed during the process (Figure 10). MAG and DAG were consecutively converted to DAG and TAG, respectively. Therefore, during the initial period, MAG is the main product; afterwards, at the end of the reaction, DAG becomes the major product [34].
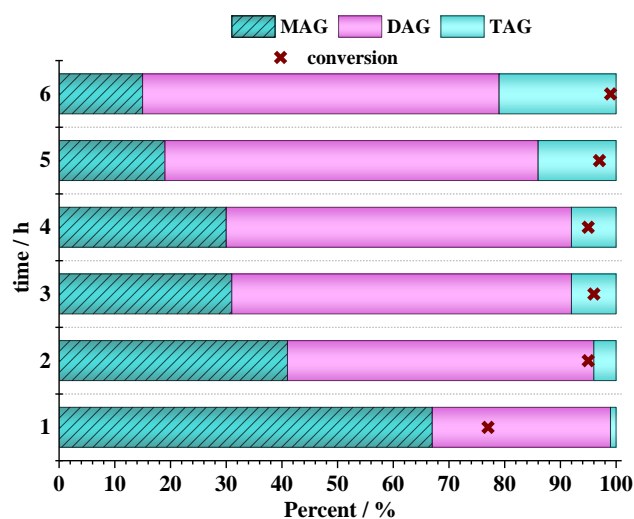

Figure 10. Effect of time on the conversion and selectivity of $H_4SiW_{12}O_{40}$/nMCM−48-catalyzed esterification of glycerol with acetic acid (adapted from ref. [34]). Reaction conditions: glycerol: HOAc molar ratio (1:6); catalyst load (50 mg); temperature (353 K).

Kim et al. assessed the activity of phosphomolybdic acid supported on different solid matrixes [52]. Figure 11 displays the results of conversion and selectivity of the reactions carried out over $H_3PMo_{12}O_{40}/SBA-15$ and $H_3PMo_{12}O_{40}/Nb_2O_5$ catalysts.
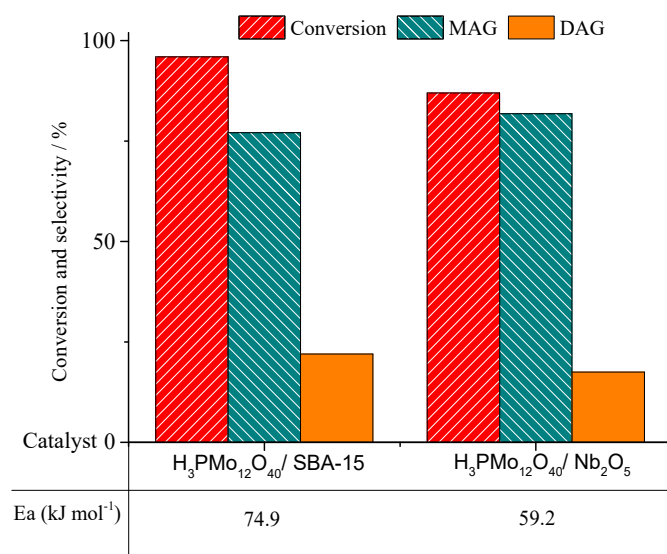
Figure 11. Conversion and selectivity of $H_3PMo_{12}O_{40}/SBA-15$ or $H_3PMo_{12}O_{40}/Nb_2O_5-$catalyzed reactions of glycerol esterification with HOAc (adapted from ref. [52]). Reaction conditions: glycerol: HOAc molar ratio (1:6); catalyst load (5 wt.%); time (8 h); temperature (353 K).

Those authors compared these results with others achieved in reactions over different solids and concluded that the strength and different nature of acid sites are important to correlating the conversions obtained. Remarkably, although the $H_3PMo_{12}O_{40}/Nb_2O_5-$catalyzed reaction presented the lowest activation energy among the various solid-catalyzed reactions, it did not reach the highest conversion after 8 h [52].

Patel and Sing investigated the effect of support $H_3PW_{12}O_{40}$ in glycerol esterification with HOAc [53]. MCM-41 and ZrO_2 were the solids selected to anchor the $H_3PW_{12}O_{40}$. Figure 12 shows the results of conversion and selectivity of the reactions carried out over $H_3PW_{12}O_{40}/MCM-41$ and $H_3PW_{12}O_{40}/ZrO_2$ catalysts.
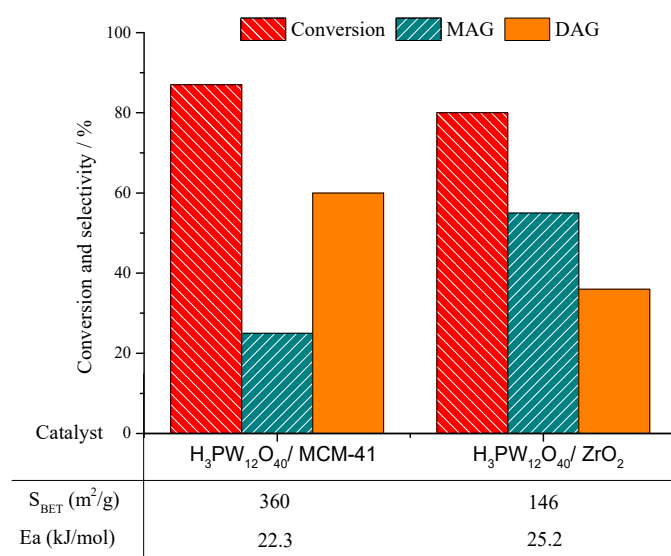
Figure 12. Conversion and selectivity of $H_3PW_{12}O_{40}/MCM-41$ or $H_3PW_{12}O_{40}/ZrO_2-$catalyzed reactions of glycerol esterification with HOAc (adapted from ref. [53]). Reaction conditions: glycerol: HOAc molar ratio (1:6); catalyst mass (150 mg); $H_3PW_{12}O_{40}$ load (30 wt.%); time (6 h); temperature (373 K).

The $H_3PW_{12}O_{40}$/MCM−41 reaction achieved the highest conversion selectivity to DAG ester. The authors ascribed the difference in conversion and selectivity to the distinct values of activation energy and the different nature of the supports [53].

2.1.2. Esterification Reactions of Glycerol over Heteropoly Salts

As verified in the reactions over solid-supported HPAs, the main reaction products of phosphotungstic acid and their silver salts were the MAG, DAG, and TAG esters (Scheme 2).
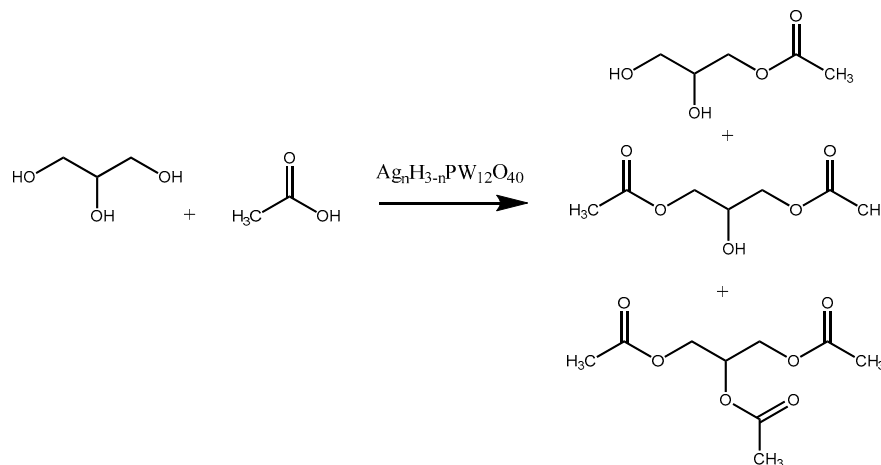
Scheme 2. Main products of the $Ag_nH_{3-n}PW_{12}O_{40}$-catalyzed glycerol esterification with acetic acid [54].

Zhu et al. synthesized silver-exchanged phosphotungstic acid salts and evaluated their catalytic activity in glycerol esterification reactions with acetic acid [54]. The conversion and selectivity reached in the $Ag_nH_{3-n}PW_{12}O_{40}$−catalyzed reactions are presented in Figure 13. Remarkably, the reaction carried out over silver partially exchanged salt $AgH_2PW_{12}O_{40}$ achieved the highest conversion (Figure 13).
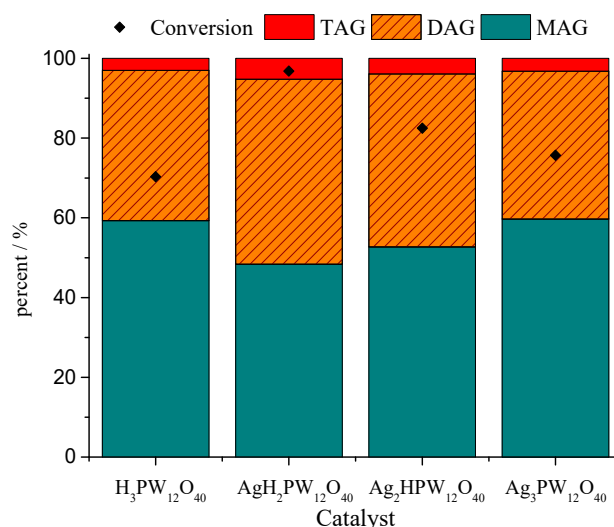

Figure 13. Conversion and selectivity of glycerol esterification reactions with acetic acid in the presence of phosphotungstic acid or their silver salts Reaction conditions: temperature (393 K); glycerol to the acetic acid molar ratio (1:10); catalyst load (1 wt.%); reaction time (15 min) (adapted from ref. [54]).

Zhu et al. concluded that the main aspects that justify the best performance of $AgH_2PW_{12}O_{40}$ catalyst in this reaction are an adequate combination of Brønsted and

Lewis acidic sites, a high tolerance to water, and a strong stability under reaction conditions (i.e., the polar solvent) [54].

In addition, Zu et al. verified that glycerol esterification with HOAc is a consecutive reaction; therefore, to maximize the yield of the bioadditives DAG and TAG, the reaction time should be extended, as unequivocally demonstrated by the selectivity data in Figure 14 [54].
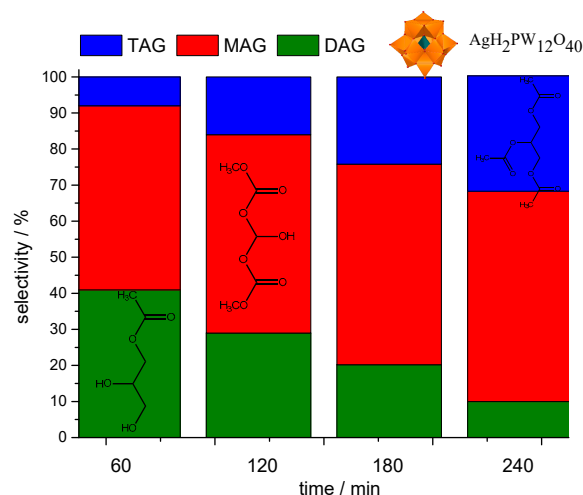

Figure 14. Impact of reaction time on the selectivity of $AgH_2PW_{12}O_{40}$−catalyzed glycerol esterification with acetic acid. Reaction conditions: temperature (393 K); glycerol/acetic acid molar proportion (1:10); catalyst loading (1 wt.%) (Adapted from ref. [54]).

This consecutive character can be explained by comparing the activation energy of these three reactions. Veluturia et al. investigated the glycerol esterification over cesium partially exchanged phosphotungstic acid salts and determined through kinetic study that this reactivity sequence is a consequence of trends observed in the activation energy of these reactions (Scheme 3) [55].
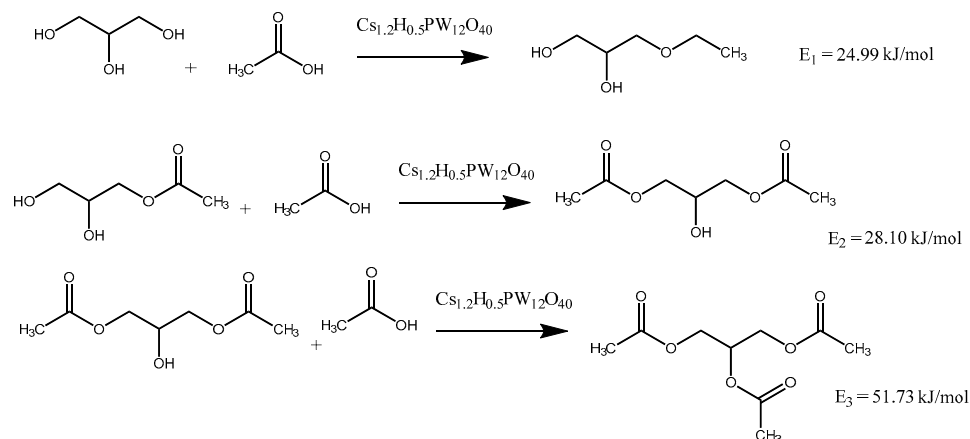
Scheme 3. The activation energy of the formation reactions of MAG, DAG, and TAG [55].

Zhu et al. also assessed the esterification of glycerol with other carboxylic acids (Figure 15) [54]. They found that an increase in the carbon chain size of an acid resulted in a lower conversion of glycerol within the studied period. Conversely, the glycerol monoester selectivity was greater for the acids with three or four carbon atoms.

Other silver heteropoly salts were too active in glycerol esterification reactions. Xu et al. synthesized silver salts of silicotungstic acid and evaluated their catalytic activity in glycerol esterification reactions with lauric acid (Scheme 4) [56].
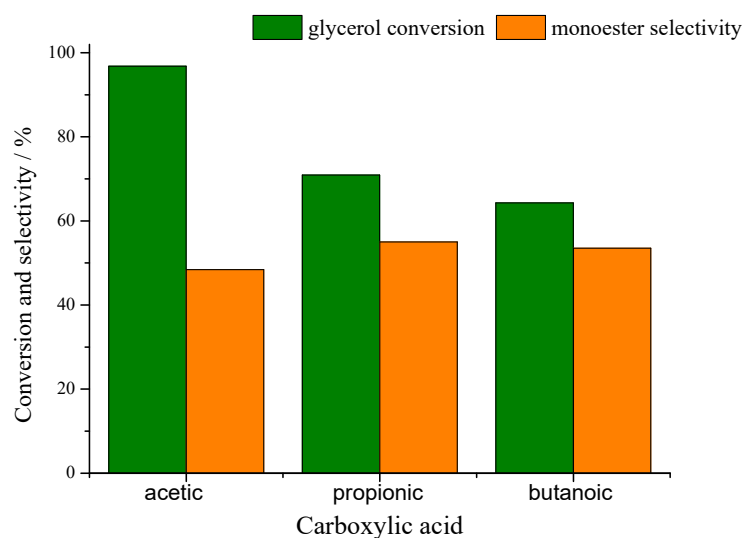
Figure 15. Esterification of glycerol with carboxylic acids (i.e., C2–C4) with a AgH$_2$PW$_{12}$O$_{40}$ catalyst (adapted from ref. [54]). Reaction conditions: temperature (393 K); alcohol/acid molar ratio (1:10); catalyst loading (1 wt.%); reaction time (15 min).

Scheme 4. Glycerol esterification with lauric acid over silver partially exchanged silicotungstate catalyst [56].

The combination of Lewis and Brønsted acid sites plays a vital role in these reactions; the runs in the presence of pristine heteropolyacid or their partially exchanged silver salts achieved conversions close to or higher than 90%, with a selectivity of 78 to 84% toward monolaurate (Figure 16).
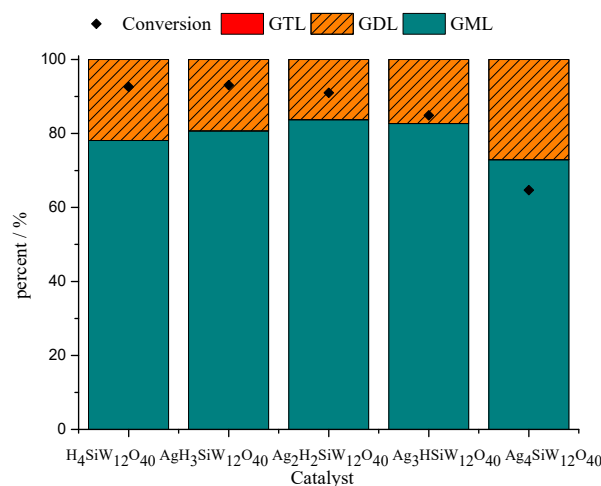

Figure 16. Catalytic performances of silicotungstic acid and their silver total or partially exchanged salts in the esterification of glycerol with lauric acid (adapted from ref. [56]). Reaction conditions: glycerol to the lauric acid molar ratio (4:1); amount of catalyst (4 wt.%); reaction time (150 min); reaction temperature (423 K).

Only the reaction in the presence of totally exchanged salt reached 70% conversion. Although the H$_3$PW$_{12}$O$_{40}$ acid achieved conversion and selectivity close to those achieved

by the mono and di silver silicotungstate, these two last acids are insoluble, an important aspect of these reactions [56].

Da Silva et al. investigated the glycerol esterification with HOAc using Sn(II) exchanged heteropoly salts (i.e., $Sn_{3/2}PW_{12}O_{40}$, $H_{3/2}PMo_{12}O_{40}$, and $Sn_2SiW_{12}O_{40}$) [57].

They verified that, in the absence of a catalyst, a poor conversion was achieved (Figure 17). Conversely, in the presence of tin(II) heteropoly salts, the conversion significantly increased. Regardless of the Keggin anion, MAG and DAG were always the main products. This superior performance of $Sn_{3/2}PW_{12}O_{40}$ can be attributed to its higher strength of acidity.
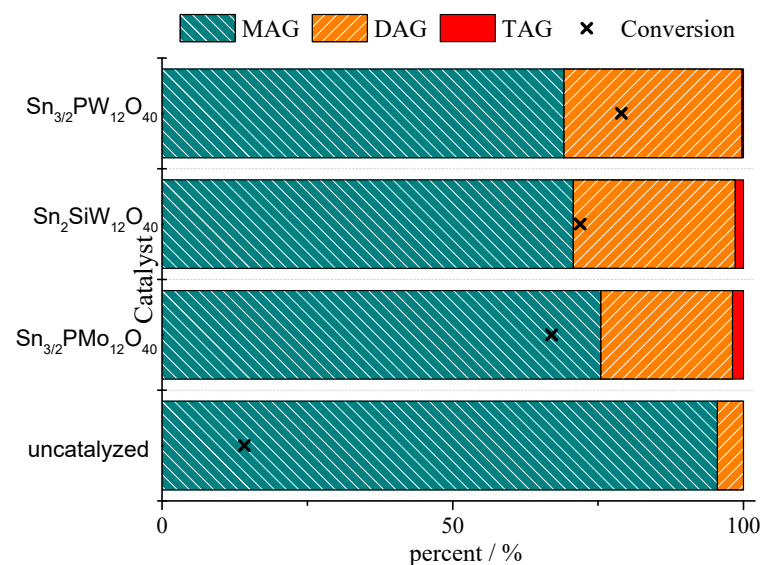

Figure 17. Tin-heteropoly-salt-catalyzed reactions: effect of the anion (adapted from ref. [57]). Reaction conditions: glycerol (24.0 mmol); HOAc (72.0 mmol); temperature (333 K); catalyst (0.10 mol % Sn^{2+}); volume (10 mL).

The $Sn_{3/2}PW_{12}O_{40}$ was the most active and selective toward MAG and DAG. Aiming to enhance the performance of the $Sn_{3/2}PW_{12}O_{40}$ catalyst, the authors thermally treated the stannous phosphotungstate salt. The main results are depicted in Figure 18.
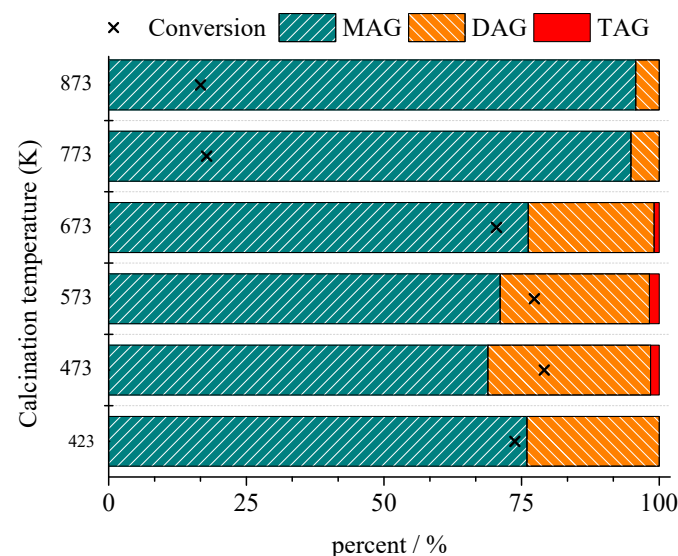
**Figure 18.** Impact of thermal treatment on the activity of $Sn_{3/2}PW_{12}O_{40}$ catalyst in esterification reactions of glycerol with HOAc (adapted from ref. [57]). Reaction conditions: glycerol (24.0 mmol); HOAc (72.0 mmol); temperature (333 K); catalyst (0.10 mol % Sn^{2+}); volume (10 mL).

The thermal treatment at 573 K of the $Sn_{3/2}PW_{12}O_{40}$ catalyst improved its catalytic performance. However, temperatures greater than 673 K led to a strong decrease in the conversion of glycerol. The authors verified that the heteropolyanion structure collapsed when it was treated at these temperatures [57].

2.2. Etherification Reactions of Glycerol

Traditionally, glyceryl ethers have been synthesized from the reaction of glycerol with isobutylene [58]. However, although highly selective, this route has as the main drawbacks the use of fossil-origin raw material and the inconvenience of the high level of polymerization undergone by the olefine at reaction conditions.

Alternatively, the use of $tert-$butyl alcohol in substitution of isobutylene dispenses additional solvents, avoiding three-phase systems and their inconvenience. Moreover, *tert*-butyl alcohol can be produced from lignocellulosic biomass, being thus a renewable origin reactant [59].

The etherification of glycerol produces compounds with a lower polarity and viscosity and, therefore, greater volatility. This gives glycerol ethers numerous applications, especially as additives for fuels and solvents. Mono-, di-, and tri-*tert*-butyl glycerol ethers (MTBG, DTBG, and TTBG, respectively) are potential fuel additives, mainly DTGB and TTGB ethers, which can be directly used in the formulation of diesel or biodiesel fuel [60]. Remarkably, these oxygenated additives can mitigate the emission of carbon monoxide, particulate matter, and unburned hydrocarbons by diesel fuel [61]. Moreover, glycerol ethers can reduce the viscosity of biodiesel, enhancing the properties of cold flow [60,61].

2.2.1. Etherification Reactions of Glycerol over Solid-Supported HPAs

DTBG and TTBG are additives that can potentially be blended either with diesel or biodiesel at 30–40%. They have been produced using different solid acid catalysts such as nanostructured zeolites [62]. However, herein we focus only on the solid-supported HPAs catalysts.

Srinivas et al. supported the cesium-exchanged phosphotungstic acids (i.e., general formulae $Cs_{3-n}H_nPW_{12}O_{40}$, n = 0, 1, 2, or 3) on tin(IV) oxide and evaluated their catalytic activity in the synthesis of glycerol ethers using *tert*-butyl alcohol as an alkylation agent (Figure 19) [63].
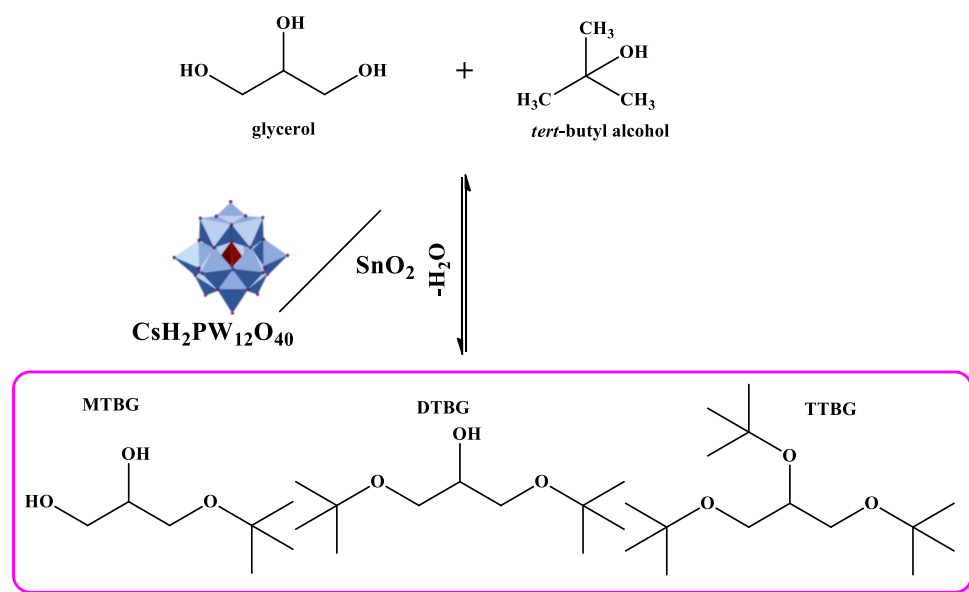

Figure 19. Etherification of glycerol with tert-butyl alcohol over $CsH_2PW_{12}O_{40}/SnO_2$ (adapted from ref. [63]).

Those authors varied the dopant loading ($CsH_2PW_{12}O_{40}$) on the SnO_2 support and evaluated the impact on the conversion and reaction selectivity (Figure 20) [63].
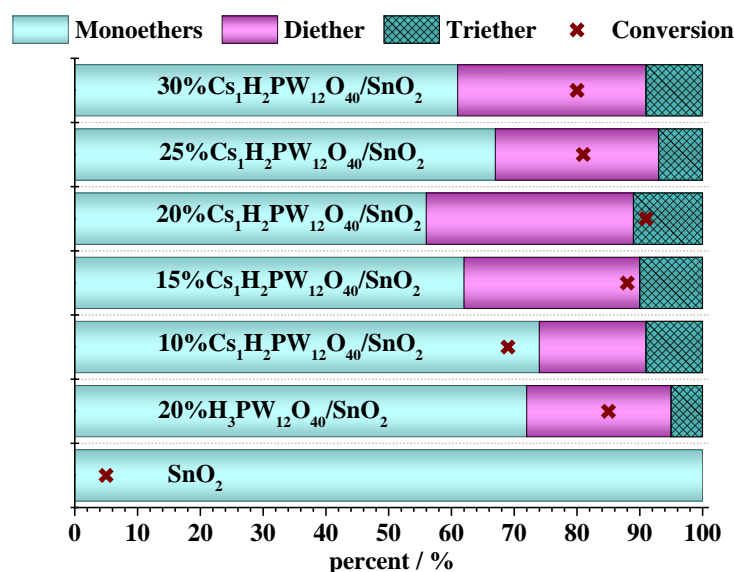

Figure 20. Impact of variation of $CsH_2PW_{12}O_{40}$ loading on the SnO_2 in the conversion and selectivity of glycerol and etherification with tert−butyl alcohol (adapted from ref. [63]. Reaction conditions: glycerol (1.84 g); *tert*−butyl alcohol (17.84 g); catalyst weight (0.5 g); reaction temperature (373 K); and reaction time (1 h).

The SnO_2 support was almost inactive in this reaction. Conversely, the doping with 10 wt.% of $CsH_2PW_{12}O_{40}$ was enough to achieve 70% conversion (Figure 20). The authors concluded that the activity of the catalyst depends on the amount of surface acidic sites and the dispersion amount of $CsH_2PW_{12}O_{40}$ over SnO_2; consequently, when a high load was used (25 or 30 wt.%), the reaction conversions were lower than those achieved with 15 or 20 wt.% (Figure 19) [63].

2.2.2. Etherification Reactions of Glycerol over Heteropoly Salts

In this topic, several processes for converting glycerol to tert-butyl ethers using *tert*-butyl alcohol over heteropoly salts are addressed. The main ethers formed are depicted in Figure 21. The steric hindrance explains why vicinal ethers were not obtained.
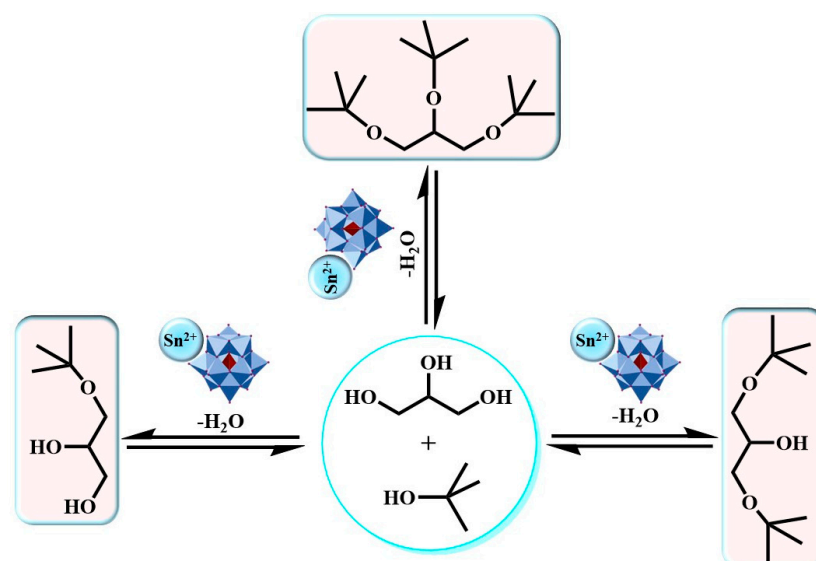

Figure 21. Main *tert*−butyl glycerol ethers obtained in the Sn(II) heteropoly salts [64].

Da Silva et al. synthesized different tin(II) heteropoly salts (i.e., phosphotungstate, phosphomolybdate, and silicotungstate) and assessed their catalytic activity in glycerol etherification reactions with *tert*−butyl alcohol [64]. Figure 22 shows a comparison of tin(II) heteropoly salt with their respective pristine heteropolyacids.
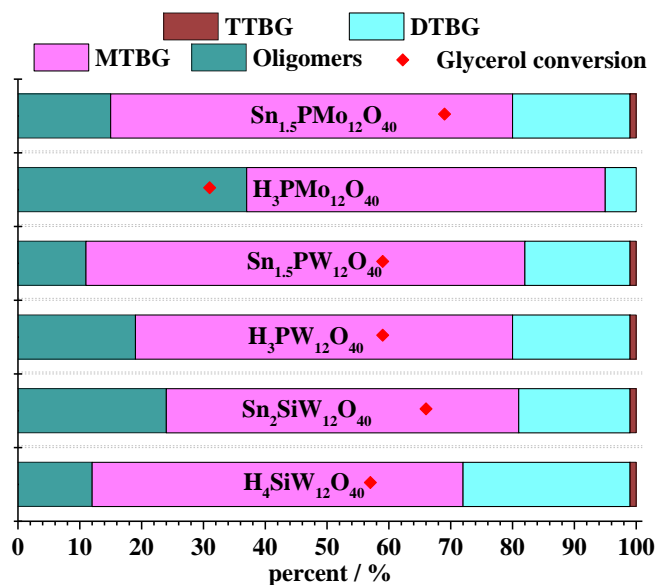

Figure 22. Conversion and selectivity of glycerol etherification reactions in the presence of Keggin heteropolyacids or their Sn^{2+} salts (adapted from ref. [64]).

Regardless of the type of Keggin anion, the heteropolyacids were less active than their tin(II) exchanged salts (Figure 22). The more noticeable effect was observed when the protons of phosphomolybdic acid were exchanged with Sn(II) cations, this salt being much more selective to ethers. At these reaction conditions, oligomers were also obtained, compromising the selectivity toward glycerol *tert*-butyl ethers.

Da Silva et al. assessed the effect of the level of exchange of the H^+ cations with Sn^{2+} on the activity of Keggin heteropoly salts in glycerol etherification reactions with *tert*-butyl alcohol [65]. The conversions and MTBG selectivity obtained in these reactions are presented in Figure 23.
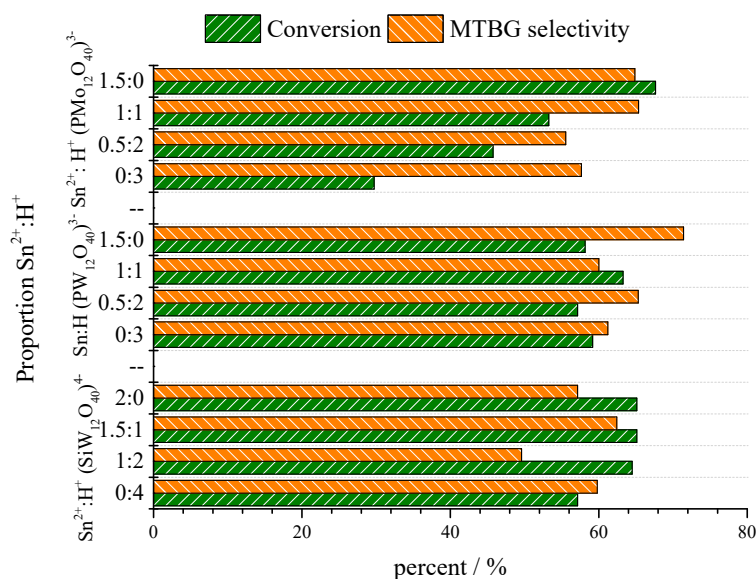

Figure 23. Impact of variation in the Sn^{2+}: H^+ proportion on the conversion and selectivity of glycerol etherification reactions with *tert*−butyl alcohol (adapted from ref. [65]).

Remarkably, the variation of the Sn^{2+}: H^+ proportion has an effect that was more noticeable in the phosphomolybdate-catalyzed reactions (Figure 23). For these catalysts, an increase in Sn load increased the conversion and MTBG selectivity [65]. The authors assigned this to the lower Brønsted acidity strength of the $H_3PMo_{12}O_{40}$ catalyst. A high tin load gives these salts more Lewis's acid sites, which compensates their weakness.

2.3. Ketalization and Acetalization Reactions of Glycerol

Acetals and ketals are substances obtained from the reaction of alcohols with aldehydes or ketones, respectively, under the action of acid catalysts. Ketals and acetals derived from glycerol have diverse applications, highlighting their use as an additive for fuels. Glycerol acetals or ketals can improve oxidation stability and reduce the pour point and the viscosity of biodiesel [66]. Solketal, a five-membered ring product of the condensation of glycerol with acetone, deserves highlighting because it reduces the formation of gum, enhances the cold flow properties, and decreases the emission of particulate material [67]. In addition, its addition to gasoline improves the octane number [68]. Several solid acid catalysts have been used to produce solketal or glycerol acetals [69]. Herein, only those based on heteropoly compounds are discussed.

2.3.1. Ketalization and Acetalization Reactions of Glycerol over Solid-Supported HPAs

Ketals or acetals are prepared from the reaction of aldehyde or ketone, respectively. This reversible reaction involves a mechanism of two steps (Scheme 5). In the first step, the protonation of the carbonyl group gives a protonated intermediate, which, after undergoing a nucleophilic attack from alcohol, releases water and the hemiacetal.
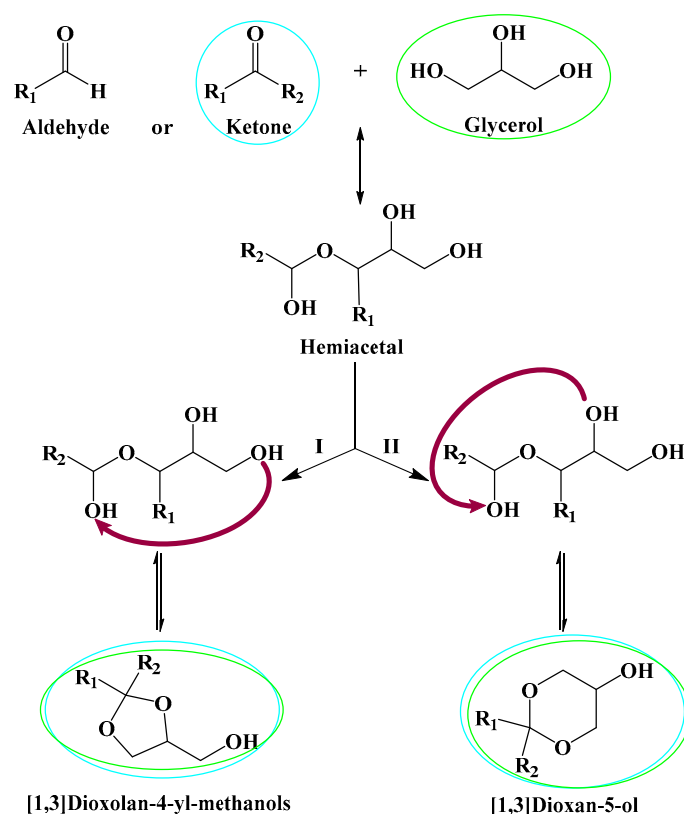
Scheme 5. Probable reaction pathway of solketal isomers [21,66].

Castanheiro et al. stated that the acetal formation is strongly impacted by electronic and steric factors [21]. Those authors verified that the rate-determining step is the formation of a cation from the protonated hemiacetal. Moreover, they suggested that the acidity strength of the medium should be enough to promote the formation of protonated

intermediates. In the second step, the hemiacetal is protonated and, after generating a protonated intermediate, gives acetal and another water molecule [21,66].

The glycerol acetalization with acetone provides two isomers as shown in Scheme 5. After the formation of hemiacetal, the intramolecular attack of the hydroxy group can happen through two pathways: the cyclization involving the secondary hydroxy group provides the five-membered ring, while the cyclization with a terminal hydroxy group leads to the six-membered ring.

Castanheiro et al. immobilized the $H_3PW_{12}O_{40}$, $H_3PMo_{12}O_{40}$, $H_4SiW_{12}O_{40}$, and $H_4SiMo_{12}O_{40}$ acids in silica by the sol-gel method and evaluated their catalytic activity in glycerol condensation with acetone to produce solketal [21].

The strongest acid catalyst, demonstrated by the highest Ei value ($H_3PW_{12}O_{40}/SiO_2$), was the most active and achieved the highest TOF. The tungstate catalysts were more acidic and consequently were more active than molybdate catalysts (Table 2) [21].

Table 2. Impact of HPA load, the strength of acidity, and surface area on the activity and TON achieved in reactions of glycerol condensation with acetone [a,b,c,d] (adapted from ref. [21]).

Catalysts	HPA Load/ wt.% [a]	TOF/ (s−) [b]	Activity/ mol/h. Catalyst [c]	Ei/ mV [d]	BET/ m² g-
$H_3PW_{12}O_{40}/SiO_2$	4.2	4.4	0.19	290	458
$H_3PMo_{12}O_{40}/SiO_2$	5.7	3.4	0.17	189	332
$H_4SiW_{12}O_{40}/SiO_2$	3.7	1.8	0.14	158	478
$H_4SiMo_{12}O_{40}/SiO_2$	3.9	1.2	0.12	137	466

[a] HPA load was determined through ICP analyses. [b] Initial activities (TOF) taken as the maximum observed reaction rate, calculated from the maximum slope of the glycerol kinetic curve. [c] Reaction conditions: glycerol to acetone molar ratio (1:6); temperature(343 K); catalyst loading (0.2 g). [d] Determined from curves of n-butylamine potentiometric titration.

Chansorn et al. prepared a catalyst based on nanodispersed $H_3PW_{12}O_{40}$ in polymer grafted on silica nanoparticles and evaluated their catalytic activity in condensation of glycerol with acetone to produce solketal [70].

Those authors verified that, regardless of reaction time, the reaction over nanodispersed $H_3PW_{12}O_{40}$ grafted on silica nanoparticles−poly(N−methyl−4−vinylpiridium) achieved always the highest solketal yield (Figure 24) [70].
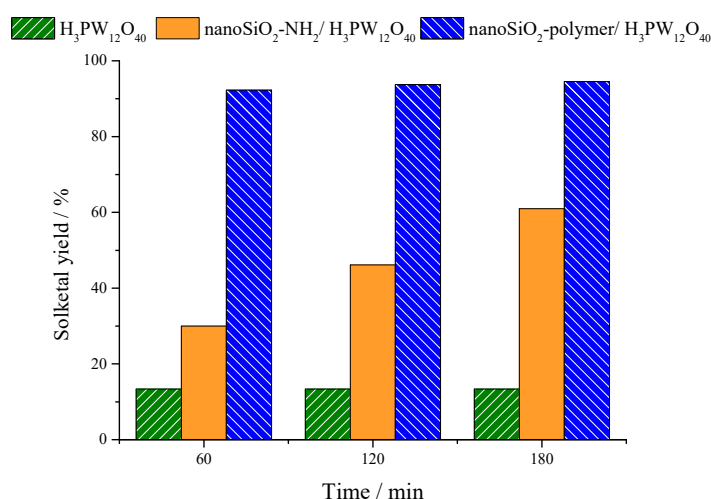
**Figure 24.** Solketal yield achieved in glycerol condensation with acetone over $H_3PW_{12}O_{40}$, nanodispersed $H_3PW_{12}O_{40}$ grafted on silica nanoparticles-NH₂, and nano-dispersed $H_3PW_{12}O_{40}$ grafted on silica nanoparticles-poly(N-methyl-4-vinylpiridium (adapted from ref. [70]). Reaction conditions: glycerol/acetone molar ratio (1:8); temperature (343 K); catalyst loading = 5.0 wt.

2.3.2. Ketalization and Acetalization Reactions of Glycerol over Heteropoly Salts

Sandesh et al. synthesized a series of organic–inorganic hybrid catalysts obtained from metathesis reactions of an organic ammonium salt and Keggin heteropoly acids and evaluated their catalytic activity in ketalization reactions of glycerol with acetone at room temperature [71]. Among the several acid solids tested, the $((C_3H_7)_4N^+)_3PW_{12}O_{40}$ was the most active and selective catalyst Scheme 6.
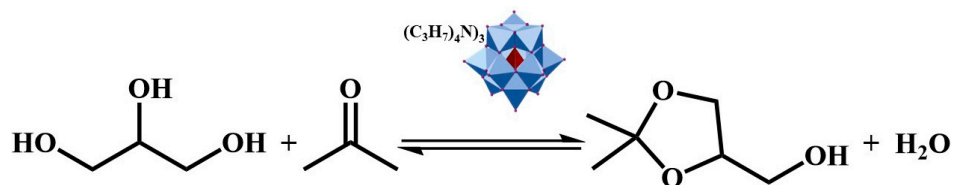
Scheme 6. $(C_3H_7)_4N^+)_3PW_{12}O_{40}$-catalyzed glycerol ketalization with acetone (adapted from ref. [71]).

Sandesh et al. investigated the impact of cationic radium on the activity of phosphotungstate salts [71]. In Figure 25, it is possible to compare the performance of ammonium-derived heteropoly catalysts. Although the $H_3PW_{12}O_{40}$-catalyzed reaction was faster than reactions in the presence of ammonium salts, it was carried out in homogeneous solutions, as this acid is soluble in acetone. The $(C_3H_7)_4N^+)_3PW_{12}O_{40}$ catalyst was easily recovered and successfully reused three times without loss of activity [71].
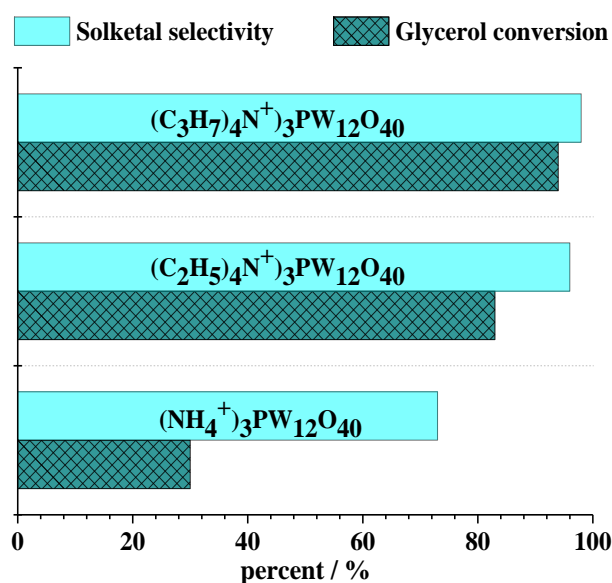

Figure 25. Catalytic activities of ammonium phosphotungstate and organic phosphotungstate salts in carbonation reactions of glycerol with urea. Reaction conditions: Glycerol: acetone molar ratio (1:6); temperature (303 K); catalyst load (3 wt% related to the glycerol); reaction time (120 min) (adapted from ref. [71]).

An increase in radium cations enhanced the conversion and reaction selectivity, consequently, the activity obeyed the following trends: $(C_3H_7)_4N^+)_3PW_{12}O_{40} > (C_2H_5)_4N^+)_3PW_{12}O_{40} > (NH_4^+)_3PW_{12}O_{40}$ [71]. Sandesh et al. also investigated the effect of a Keggin heteropolyanion on the catalyst activity (Figure 26).

The *tert*-butyl ammonium phosphotungstate salt was the most active catalyst, reaching the highest TON. These data are suggestive that the Keggin heteropolyanion's nature had a minor role in these reactions.
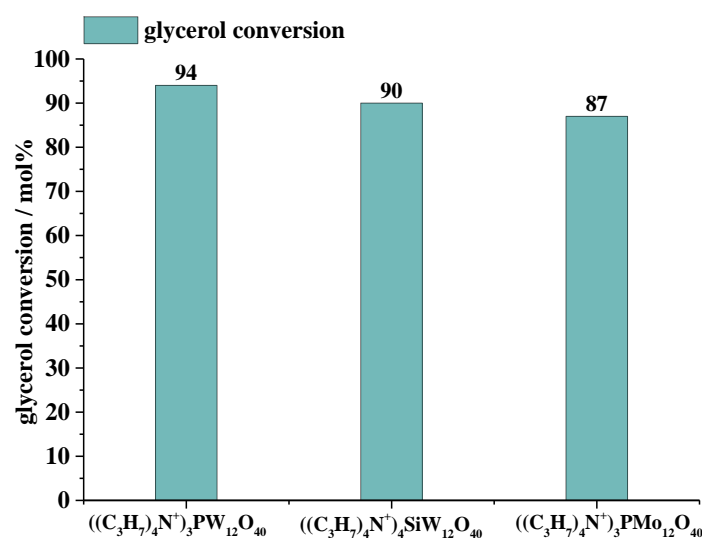
Figure 26. Impact of the Keggin anion on the catalytic activity of organic–inorganic heteropoly salts in carbonation reactions of glycerol with urea (adapted from ref. [71]).

Da Silva et al. assessed the activity of tin(II) silicotungstate on the acetalization of glycerol with acetone [72]. The impact of the main reaction variables was assessed. Figure 27 shows the effect of the proportion of acetone to glycerol on the reaction conversion. The authors verified that an increase in acetone load enhanced the conversion of the reactions. This is a reversible reaction, and an acetone excess shifts the equilibrium toward ketal formation.
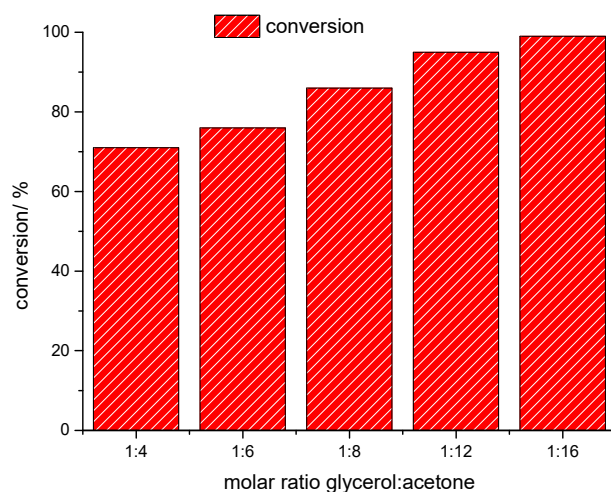

Figure 27. The impacts of variation on the stoichiometry of reactants on $Sn_2SiW_{12}O_{40}$-catalyzed glycerol condensation with acetone (adapted from ref. [72]). Reaction conditions: glycerol: acetone (variable); volume (10 mL); catalyst (0.01 mol%); 298 K.

The impact of catalyst load was also assessed (Figure 28). An increase in catalyst load of 1×10^{-3} to 6.0×10^{-3} mol% had a positive effect; however, greater loads did not trigger significant changes, since the reaction had achieved the maximum conversion.

Da Silva et al. investigated the glycerol acetalization with acetone in a homogenous phase using various metal cations to replace the protons of silicotungstic acid [73]. Although these salts are solid when pure, in the presence of solvent, they are soluble because they have a cationic radium smaller than 1.3 Angstrom. Therefore, all these reactions happen in a homogeneous phase. The reaction conversions are shown in Figure 29.
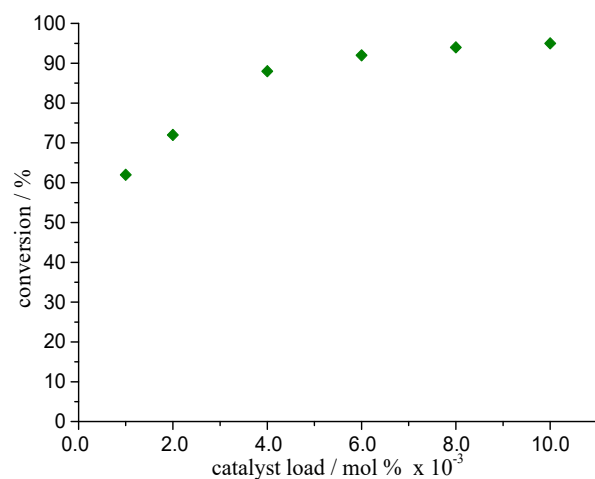
Figure 28. The effects of catalyst load on the kinetic curves of $Sn_2SiW_{12}O_{40}$−catalyzed glycerol condensation with acetone (adapted from ref. [72]. Reaction conditions: glycerol: acetone (1:12); volume (10 mL); $Sn_2SiW_{12}O_{40}$ catalyst (variable); 298 K.
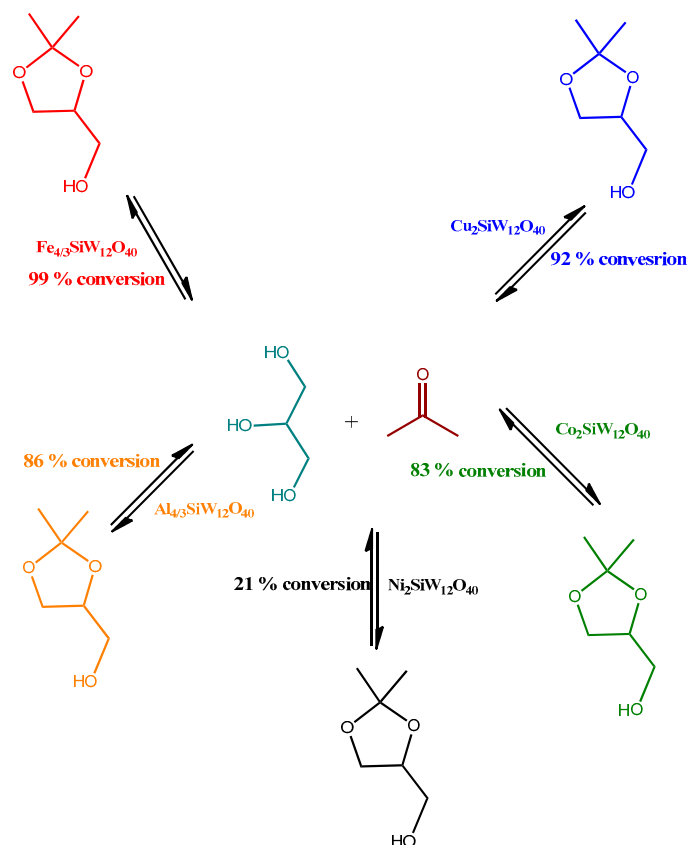
Figure 29. Synthesis of solketal catalyzed by metal-exchanged silicotungstic acid salts (adapted from ref. [73]).

Among the reactions tested, the one performed in the presence of $Fe_{4/3}SiW_{12}O_{40}$ salt reached the highest glycerol conversion. Measurements of pH in the reaction medium showed that this heteropoly salt triggered the highest increase in acidity of the reaction medium [73]. Impacts of variation in glycerol to acetone proportion and $Fe_{4/3}SiW_{12}O_{40}$ catalyst load were also investigated (Figure 30; Figure 31, respectively).
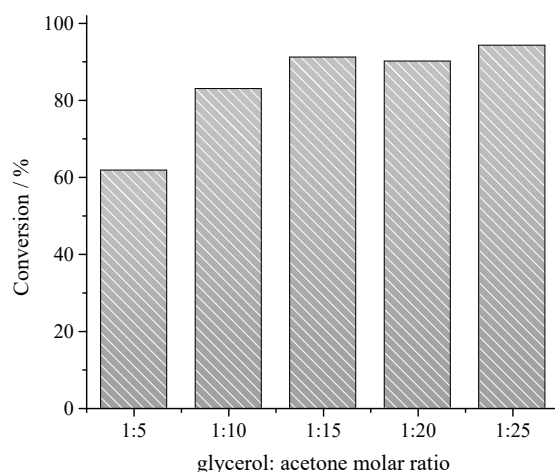
Figure 30. Impact of the glycerol: acetone molar ratio on the conversion of $Fe_{4/3}SiW_{12}O_{40}-$ catalyzed glycerol ketalization with acetone (adapted from ref. [73]). Reaction conditions: glycerol: acetone (variable); temperature (298 K); $Fe_{4/3}SiW_{12}O_{40}$ catalyst (0.30 mol%); volume (10 mL); and reaction time (1 h).
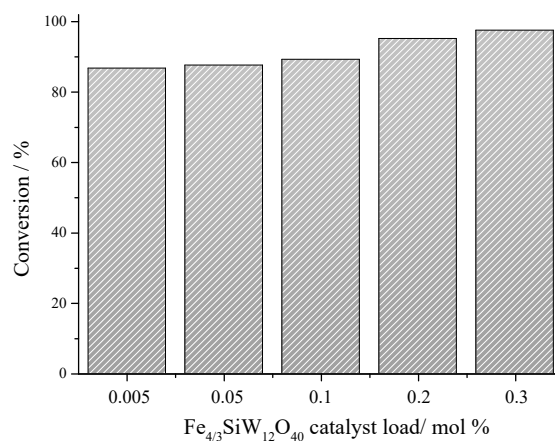
Figure 31. Impact of the $Fe_{4/3}SiW_{12}O_{40}$ catalyst load on the conversion of glycerol ketalization with acetone (adapted from ref. [73]). Reaction conditions: glycerol: acetone (variable); temperature (298 K); $Fe_{4/3}SiW_{12}O_{40}$ catalyst (0.30 mol%); volume (10 mL); and reaction time (1 h).

An increase in acetone load led to a higher conversion of glycerol (Figure 30). Although omitted herein, the solketal selectivity was greater than 90% in all of the reactions.

The $Fe_{4/3}SiW_{12}O_{40}-$ catalyzed glycerol ketalization reactions showed that high TON was achieved even when the lowest catalyst load was used. This is evidence of the high activity of this heteropoly salt.

2.4. Carbonatation Reactions of Glycerol

Glycerol carbonate has several industrial applications, being used to produce solvents, polycarbonates, polyesters, polyurethanes, and polyamides. The most environmentally benign route to produce this compound involves the reaction of glycerol with urea [74].

Carbonatation Reactions of Glycerol over HPA Catalysts

Srikanth et al. prepared a series of solid Cs-exchanged phosphotungstic acid salt catalysts impregnated with $Sn(NO_3)_2$ and evaluated their catalytic activity in glycerol carbonation reactions with urea [75].

The reactions carried out over gave as main products glycerol carbonate (I), glycidol (II), and glycerol urethane (III), as described in the reaction pathway in Figure 32. Although

all the catalysts were calcined to 773 K, no decomposition of the Keggin anion was noticed; however, certainly, the $Sn(NO_3)_2$ was decomposed to SnO and/or SnO_2.
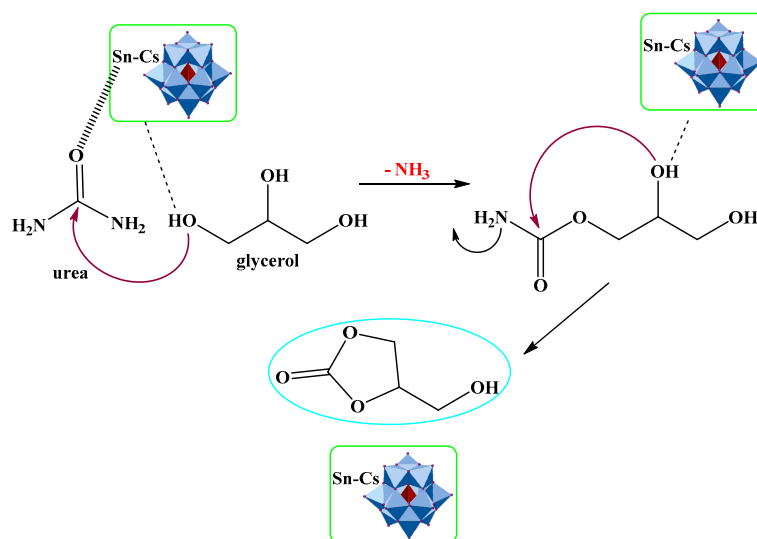
Figure 32. Main products of glycerol carbonation with urea over $Cs_3PW_{12}O_{40}$/SnO catalyst (adapted from ref. [75]).

In Figure 33 the conversion and selectivity achieved in reactions with a different molar ratio of Sn to $Cs_3PW_{12}O_{40}$ are shown. The impregnation of cesium salt with Sn led to an increase in the conversion of glycerol; the highest conversion (91%) and glycerol carbonate selectivity (83%) were achieved using a 3:1 ratio of Sn to $Cs_3PW_{12}O_{40}$. However, this happened only until the 3:1 proportion; above this proportion, there was a decrease in the conversion.
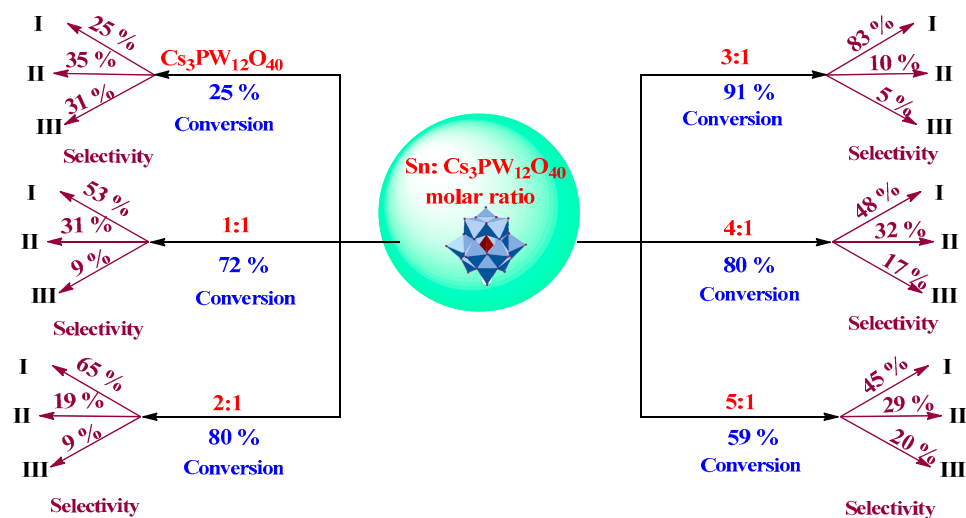
Figure 33. Impact of mora ratio of Sn to $Cs_3PW_{12}O_{40}$ on the conversion and selectivity of glycerol carbonation with urea (adapted from ref. [75]).

Srikanth et al. also investigated the effect of reaction temperature on the conversion and selectivity of glycerol carbonation with urea (Figure 34) [75].

At temperatures lower than 413 K (i.e., 393 K), both conversion and selectivity toward glycerol carbonate were diminished; the same happened at greater temperatures (433 K); however, this was due to the urea decomposition (Figure 35).
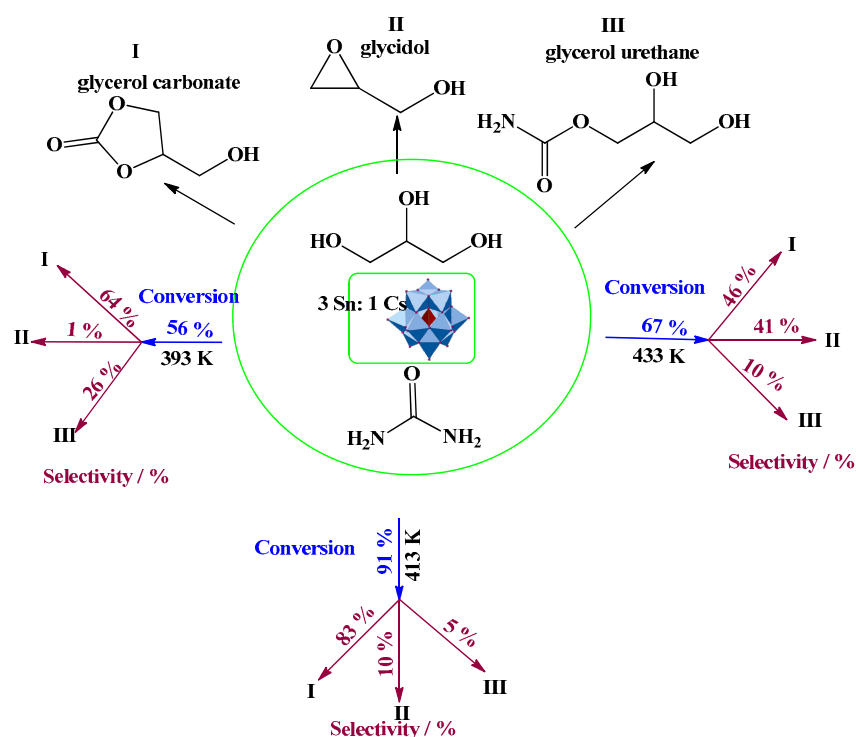
Figure 34. Impact of temperature on the conversion and selectivity of $Sn/Cs_3PW_{12}O_{40}$−catalyzed glycerol carbonation with urea (adapted from ref. [75]).
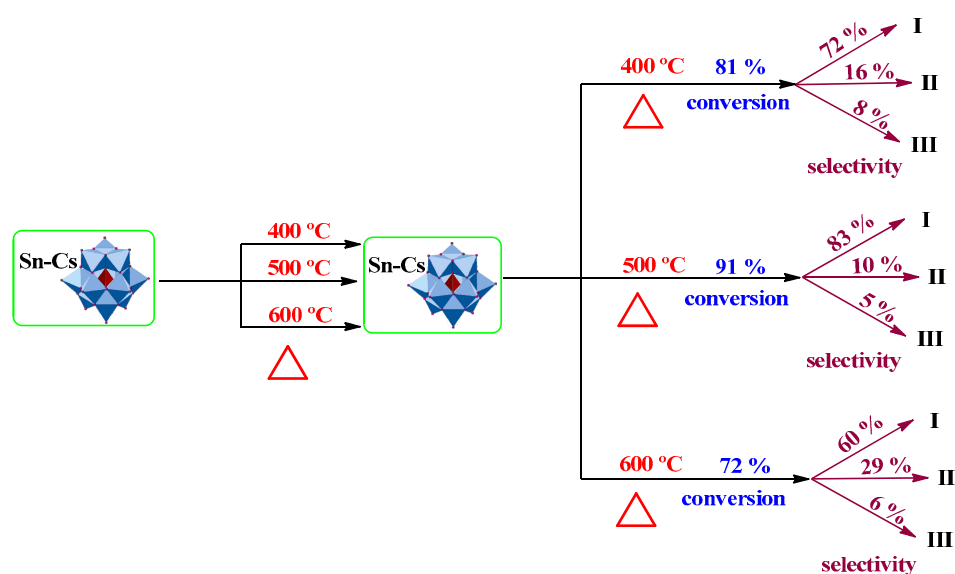
Figure 35. Effect of calcination temperature of $Sn/Cs_3PW_{12}O_{40}$ (3 Sn: 1 Cs) catalyst on the conversion and selectivity of catalyzed glycerol carbonation with urea (adapted from ref. [75]).

The $Sn/Cs_3PW_{12}O_{40}$ catalyst, when calcinated at temperatures higher than 773 K, has the Keggin anion collapsed and consequently loses catalytic activity (Figure 36). Srikanth et al. investigated the effect of Keggin anion type on the catalytic activity of Sn/Cs−HPAs solid catalysts (Scheme 7) [75].

Regardless of the Keggin anion, glycerol carbonate was always the main product. However, among the three types of tin-impregnated cesium heteropoly salts, the phospho-tungstate salt was the most active and selective toward the goal product.
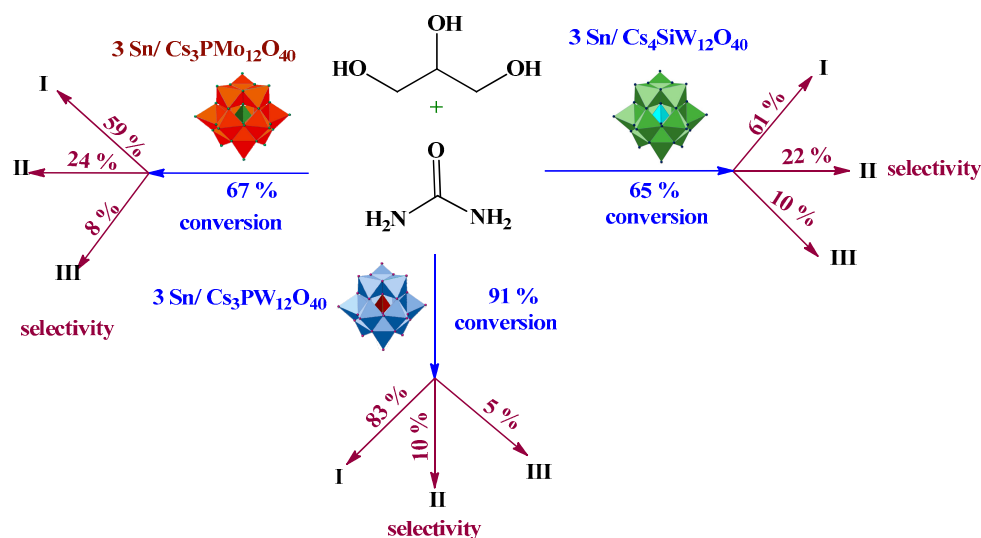
Figure 36. Effect of the Keggin anion on the conversion and selectivity of glycerol carbonatation with urea over Sn/Cs supported solid catalysts (adapted from ref. [75]).
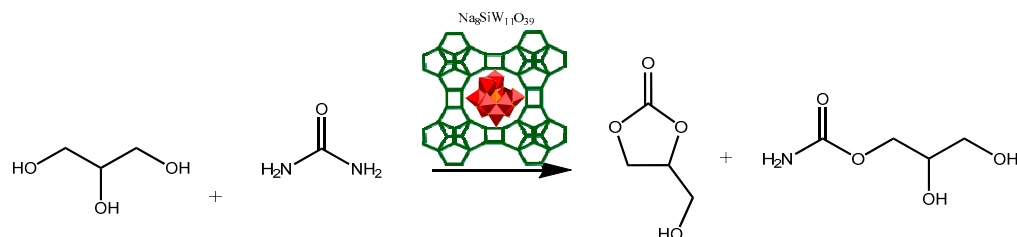
Scheme 7. NaSiW$_{11}$O$_{39}$/zeolite-catalyzed carboxylation of glycerol with urea [76].

Patel et al. synthesized salt lacunar NaSiW$_{11}$O$_{39}$ and supported it on the Hβ zeolite [76]. This catalyst was evaluated in the carbonation of glycerol with urea (Scheme 7). Table 3 summarizes the main results of reactions.

Table 3. Effect of % NaSiW$_{11}$O$_{39}$ loading on zeolite using a 1:1 proportion of glycerol to urea; time, 8 h; temperature, 413 K; catalyst amount, 100 mg. (adapted from ref. [76]).

| Loading/%	Conversion/%	Selectivity/%		
		GlyC	**GlyU**	**Others**
10	12.2	77.5	18.2	4.3
20	42.6	74.5	16.6	8.9
30	59.3	78.2	10.6	11.2
40	62.3	67.7	14.0	18.3

An increase in catalyst load enhanced the glycerol conversion; however, the selectivity toward glycerol carbonate was gradually reduced. Glycerol oligomers namely as "others" were possibly favored by a higher catalyst load.

The Keggin heteropolyacid salts rise as a very nice option to synthesize bioadittives, as solid-supported catalysts or as solid salts. They efficiently catalyze the esterification, etherification, acetalization, ketalization, and carbonylation reactions of platform molecules such as glycerol, a biodiesel byproduct. Their versatility allows their use to produce either biofuels or bioadditives. In particular, liquid-phase reactions under mild conditions achieve high conversions and selectivity toward the goal products in the presence of Keggin heteropolyacid salts in nature or with solid support.

3. Conclusions

The recent advances achieved in the glycerol conversion processes to bioadditives over solid Keggin heteropolyacid catalysts were described. The processes selected to synthesize bioadditives were esterification, etherification, acetalization, ketalization, and carbonation of glycerol. The reactions over two types of solid catalysts were addressed: solid-supported Keggin HPAs and solid heteropoly salts. A comparison of the main results achieved in these two types of processes shows that Keggin heteropolyacids are efficient catalysts either when solid-supported or when converted to solid heteropoly salts. Most of these solid catalysts are easily recovered and reused without loss of activity. It was possible to note that only the processes of glycerol carbonation still have a few routes where Keggin HPAs have been used.

Author Contributions: Conceptualization, M.J.d.S.; methodology, M.J.d.S.; software, M.J.d.S., N.P.G.L. and A.A.R.; investigation, M.J.d.S., N.P.G.L. and A.A.R.; resources, M.J.d.S., N.P.G.L. and A.A.R.; writing—original draft preparation, M.J.d.S.; writing—review and editing, M.J.d.S.; supervision, M.J.d.S. All authors have read and agreed to the published version of the manuscript.

Data Availability Statement: Not applicable.

Conflicts of Interest: The authors declare no conflict of interest.

References

1. Helwani, Z.; Othman, M.R.; Aziz; Fernando, W.J.N.; Kim, J. Technologies for production of biodiesel focusing on green catalytic techniques: A review. *Fuel Process. Technol.* **2009**, *90*, 1502–1514. [CrossRef]
2. Bozbas, K. Biodiesel as an alternative motor fuel: Production and policies in the European Union. *Renew. Sustain. Energy Rev.* **2008**, *12*, 542–552. [CrossRef]
3. Meher, L.C.; Sagar, D.V.; Naik, S.N. Technical aspects of biodiesel production by transesterification—A Review. *Renew. Sustain. Energy Rev.* **2006**, *10*, 248–268. [CrossRef]
4. Karinen, R.S.; Krause, A.O.I. New biocomponents from glycerol. *Appl. Catal. A* **2006**, *306*, 128–133. [CrossRef]
5. Sedghi, R.; Shahbeik, H.; Rastegari, H.; Rafiee, S.; Peng, W.; Nizami, A.-S.; Gupta, V.K.; Chen, W.-H.; Lam, S.S.; Pan, J.; et al. Turning biodiesel glycerol into oxygenated fuel additives and their effects on the behavior of internal combustion engines: A comprehensive systematic review. *Renew. Sustain. Energy Rev.* **2022**, *167*, 112805. [CrossRef]
6. Manara, P.; Zabaniotou, A. Co-valorization of crude glycerol waste streams with conventional and/or renewable fuels for power generation and industrial symbiosis perspectives. *Waste Biomass Valorization* **2016**, *7*, 135–150. [CrossRef]
7. Nda-Umar, U.I.; Ramli, I.; Taufiq-Yap, Y.H.; Muhamad, E.N. An overview of recent research in the conversion of glycerol into biofuels, fuel additives and other biobased chemicals. *Catalysts* **2019**, *9*, 15. [CrossRef]
8. He, Q.; McNutt, J.; Yang, J. Utilization of the residual glycerol from biodiesel production for renewable energy generation. *Renew. Sustain. Energy Rev.* **2017**, *71*, 63–76. [CrossRef]
9. Cavalcante, K.S.B.; da Silva, M.G.S.; Sifronio, F.S.M.; Valois, R.R.S.; Maciel, A.P.; Souza, A.G.; Silva, F.C. Oxygenated glycerol derivatives as an alternative source of energy: A review. *Eclet. Quím.* **2011**, *36*, 54–61. [CrossRef]
10. Nanda, M.R.; Yuan, Z.; Qin, W.; Ghaziaskar, H.R.; Poirer, M.A.; Xu, C.C. Thermodynamic and kinetic studies of a catalytic process to convert glycerol into solketal as an oxygenated fuel additive. *Fuel* **2014**, *117*, 470–477. [CrossRef]
11. Suriyaprapadilok, N.; Kitiyanan, B. Synthesis of solketal from glycerol and its reaction with benzyl alcohol. *Energy Procedia* **2011**, *9*, 63–69. [CrossRef]
12. Trifoi, A.R.; Agachi, P.S.; Pap, T. Glycerol acetals and ketals as possible diesel additives. a review of their synthesis protocols. *Renew. Sustain. Energy Rev.* **2016**, *62*, 804–814. [CrossRef]
13. Akinnawo, C.A.; Mosia, L.; Alimi, O.A.; Oseghale, C.O.; Fapojuwo, D.P.; Bingwa, N.; Meijboom, R. Eco-friendly synthesis of valuable fuel bio-additives from glycerol. *Catal. Commun.* **2021**, *152*, 106287–106293. [CrossRef]
14. Ruiz, V.E.; Velty, A.; Santos, L.L.; Perez, L.A.; Sabater, M.J.; Iborra, S.; Corma, A. gold catalysts and solid catalysts for biomass transformations: Valorization of glycerol and glycerol—Water mixtures through formation of cyclic acetals. *J. Catal.* **2010**, *271*, 351–357. [CrossRef]
15. Ballotin, F.C.; da Silva, M.J.; Teixeira, A.P.C.; Lago, R.M. Amphiphilic acid carbon catalysts produced by bio-oil sulfonation for solvent-free glycerol ketalization. *Fuel* **2020**, *274*, 117779. [CrossRef]
16. Da Silva, M.J.; de Ávila Rodrigues, F.; Júlio, A.A. SnF_2-catalyzed glycerol ketalization: A friendly environmentally process to synthesize solketal at room temperature over on solid and reusable Lewis acid. *Chem. Eng. J.* **2017**, *307*, 828–835. [CrossRef]

17. Souza, T.E.; Padula, I.D.; Teodoro, M.M.G.; Chagas, P.; Resende, J.M.; Souza, P.P.; Oliveira, L.C.A. Amphiphilic property of niobium oxyhydroxide for waste glycerol conversion to produce solketal. *Catal. Today* **2015**, *254*, 83–89. [CrossRef]

18. Okoye, P.U.; Abdullah, A.Z.; Hameed, B.H. Synthesis of oxygenated fuel additives via glycerol esterification with acetic acid over bio-derived carbon catalyst. *Fuel* **2017**, *209*, 538–544. [CrossRef]

19. Reinoso, D.M.; Tonetto, G.M. Bioadditives synthesis from selective glycerol esterification over acidic ion exchange resin as catalyst. *J. Environ. Chem. Eng.* **2018**, *6*, 3399–3407. [CrossRef]

20. Deutsch, J.; Martin, A.; Lieske, H. Investigation on heterogeneously catalyzed condensation of glycerol to cyclic acetals. *J. Catal.* **2007**, *245*, 428–435. [CrossRef]

21. Ferreira, P.; Fonseca, I.M.; Ramos, A.M.; Vital, J.; Castanheiro, J.E. Valorization of glycerol by condensation with acetone over silica-included heteropolyacids. *Appl. Catal. B Environ.* **2010**, *98*, 94–99. [CrossRef]

22. Neves, P.; Russo, P.A.; Fernandes, A.; Antunes, M.M.; Farinha, J.; Pillinger, M.; Ribeiro, M.F.; Castanheiro, J.E.; Valente, A.A. Mesoporous zirconia-based mixed oxides as versatile acid catalysts for producing bio-additives from furfuryl alcohol and glycerol. *Appl. Catal. A* **2014**, *487*, 148–157. [CrossRef]

23. Khayoon, M.S.; Triwahyono, S.; Hameed, B.H.; Jalil, A.A. Improved production of fuel oxygenates via glycerol acetylation with acetic acid. *Chem. Eng. J.* **2014**, *243*, 473–484. [CrossRef]

24. Kaur, J.; Sarma, A.K.; Jha, M.K.; Gera, P. Valorization of crude glycerol to value-added products: Perspectives of process technology, economics, and environmental issues. *Biotechnol. Rep.* **2020**, *27*, e00487. [CrossRef] [PubMed]

25. Abida, K.; Ali, A. A review on catalytic role of heterogeneous acidic catalysts during glycerol acetylation to yield acetins. *J. Indian Chem. Soc.* **2022**, *99*, 100459. [CrossRef]

26. Da Silva, M.J.; Liberto, N.A. Soluble and solid supported Keggin heteropolyacids as catalysts in reactions for biodiesel production: Challenges and recent advances. *Curr. Org. Chem.* **2016**, *20*, 1263–1283. [CrossRef]

27. Narkhede, N.; Patel, A. Biodiesel production by esterification of oleic acid and transesterification of soybean oil using a new solid acid catalyst comprising 12-tungstosilicic acid and zeolite Hβ. *Ind. Eng. Chem. Res.* **2013**, *52*, 13637–13644. [CrossRef]

28. Narkhede, N.; Patel, A. Efficient synthesis of biodiesel over a recyclable catalyst comprising a monolacunary silicotungstate and zeolite Hβ. *RSC Adv.* **2014**, *4*, 64379–64387. [CrossRef]

29. Da Silva, M.J.; Lopes, N.P.G.; Bruziquesi, C.G.O. Furfural acetalization over Keggin heteropolyacid salts at room temperature: Effect of cesium doping. *React. Kinet. Mech. Catal.* **2021**, *133*, 913–931. [CrossRef]

30. Coronel, N.C.; da Silva, M.J. Lacunar Keggin heteropolyacid salts: Soluble, solid, and solid-supported catalysts. *J. Clust. Sci.* **2018**, *29*, 195–205. [CrossRef]

31. Da Silva, M.J.; Lopes, N.P.G.; Ferreira, S.O.; da Silva, R.C.; Natalino, R.; Chaves, D.M.; Texeira, M.G. Monoterpenes etherification reactions with alkyl alcohols over cesium partially exchanged Keggin heteropoly salts: Effects of catalyst composition. *Chem. Pap.* **2021**, *75*, 153–168. [CrossRef]

32. Da Silva, M.J.; da Silva Andrade, P.H.; Sampaio, V.F.C. Transition metal-substituted potassium silicotungstate salts as catalysts for oxidation of terpene alcohols with hydrogen peroxide. *Catal. Lett.* **2021**, *151*, 2094–2106. [CrossRef]

33. Melero, J.A.; van Grieken, R.; Morales, G.; Paniagua, M. Acidic mesoporous silica for the acetylation of glycerol: Synthesis of bioadditives to petrol fuel. *Energy Fuels* **2007**, *21*, 1782–1791. [CrossRef]

34. Pithadia, D.; Patel, A. 12-Tungstosilicic acid anchored to nano-porous MCM-48: A sustainable catalyst for the valorization of bioplatform molecules to value added products. *Waste Biomass Valorization* **2022**. [CrossRef]

35. Rahmat, N.; Abdullah, A.Z.; Mohamed, A.R. Recent progress on innovative and potential technologies for glycerol transformation into fuel additives: A critical review. *Renew. Sustain. Energy Rev.* **2010**, *14*, 987–1000. [CrossRef]

36. Liu, X.; Ma, H.; Wu, Y.; Wang, C.; Yang, M.; Yan, P.; Welz-Biermann, U. Esterification of glycerol with acetic acid using double SO_3H-functionalized ionic liquids as recoverable catalysts. *Green Chem.* **2011**, *13*, 697. [CrossRef]

37. Gonçalves, C.E.; Laier, L.O.; Cardoso, A.L.; da Silva, M.J. Bioadditive synthesis from $H_3PW_{12}O_{40}$-catalyzed glycerol esterification with HOAc under mild reaction conditions. *Fuel Process. Technol.* **2012**, *102*, 46–52. [CrossRef]

38. Khayoon, M.S.; Hameed, B.H. Acetylation of glycerol to biofuel additives over sulfated activated carbon catalyst. *Bioresour. Technol.* **2011**, *102*, 9229–9235. [CrossRef]

39. Gonçalves, V.L.C.; Pinto, B.P.; Silva, J.C.; Mota, C.J.A. Acetylation of glycerol catalyzed by different solid acids. *Catal. Today* **2008**, *133–135*, 673–677. [CrossRef]

40. Liao, X.; Zhu, Y.; Wang, S.-G.; Li, Y. Producing triacetylglycerol with glycerol by two steps: Esterification and acetylation. *Fuel Process. Technol.* **2009**, *90*, 988–993. [CrossRef]

41. Okuhara, T. Water-tlerant solid acid catalysts. *Chem. Rev.* **2002**, *102*, 3641–3666. [CrossRef]

42. Pizzio, L.R.; Blanco, M.N. A contribution to the physicochemical characterization of nonstoichiometric salts of tungstosilicic acid. *Microporous Mesoporous Mater.* **2007**, *103*, 40–47. [CrossRef]

43. Gopinath, S.; Kumar, P.V.; Kumar, P.S.M.; Arafath, K.A.Y.; Sivanesan, S.; Baskaralingam, P. Cs-tungstosilicic acid/Zr-KIT-6 for esterification of oleic acid and transesterification of non-edible oils for green diesel production. *Fuel* **2018**, *234*, 824–835. [CrossRef]

44. Grinenval, E.; Rozanska, X.; Baudouin, A.; Berrier, E.; Delbecq, F.; Sautet, P.; Basset, J.-M.; Lefebvre, F. Controlled interactions between anhydrous Keggin-type heteropolyacids and silica support: Preparation and characterization of well-defined silica-supported polyoxometalate species. *J. Phys. Chem. C* **2010**, *114*, 19024–19034. [CrossRef]

45. Zhu, S.; Zhu, Y.; Gao, X.; Mo, T.; Zhu, Y.; Li, Y. Production of bioadditives from glycerol esterification over zirconia supported heteropolyacids. *Bioresour. Technol.* **2013**, *130*, 45–51. [CrossRef] [PubMed]

46. Balaraju, M.; Nikhitha, P.; Jagadeeswaraiah, K.; Srilatha, K.; Sai Prasad, P.S.; Lingaiah, N. Acetylation of glycerol to synthesize bioadditives over niobic acid supported tungstophosphoric acid catalysts. *Fuel Process. Technol.* **2010**, *91*, 249–253. [CrossRef]

47. Ferreira, P.; Fonseca, I.M.; Ramos, A.M.; Vital, J.; Castanheiro, J.E. Esterification of glycerol with acetic acid over dodecamolyb-dophosphoric acid encaged in USY zeolite. *Catal. Commun.* **2009**, *10*, 481–484. [CrossRef]

48. Ferreira, P.; Fonseca, I.M.; Ramos, A.M.; Vital, J.; Castanheiro, J.E. Acetylation of glycerol over heteropolyacids supported on activated carbon. *Catal. Commun.* **2011**, *12*, 573–576. [CrossRef]

49. Jagadeeswaraiah, K.; Balaraju, M.; Prasad, P.S.S.; Lingaiah, N. Selective esterification of glycerol to bioadditives over heteropoly tungstate supported on Cs-containing zirconia catalysts. *Appl. Catal. A* **2010**, *386*, 166–170. [CrossRef]

50. Ferreira, P.; Fonseca, I.M.; Ramos, A.M.; Vital, J.; Castanheiro, J.E. Glycerol acetylation over dodecatungstophosphoric acid immobilized into a silica matrix as the catalyst. *Appl. Catal. B Environ.* **2009**, *91*, 416–422. [CrossRef]

51. Magar, S.; Mohanraj, G.T.; Jana, S.K.; Rode, C.V. Synthesis, and characterization of supported heteropoly acid: Efficient solid acid catalyst for glycerol esterification to produce biofuel additives. *Inorg. Nano-Met. Chem.* **2020**, *50*, 1157–1165. [CrossRef]

52. Kim, I.; Kim, J.; Lee, D. A comparative study on catalytic properties of solid acid catalysts for glycerol acetylation at low temperatures. *Appl. Catal. B* **2014**, *148–149*, 295–303. [CrossRef]

53. Patel, A.; Singh, S. A green and sustainable approach for esterification of glycerol using 12-tungstophosphoric acid Anchored to different supports: Kinetics and effect of support. *Fuel* **2014**, *118*, 358–364. [CrossRef]

54. Zhu, S.; Gao, X.; Dong, F.; Zhu, Y.; Zheng, H.; Li, Y. Design of a highly active silver-exchanged phosphotungstic acid catalyst for glycerol esterification with acetic acid. *J. Catal.* **2013**, *306*, 155–163. [CrossRef]

55. Veluturia, S.; Narula, A.; Rao, D.S.; Shetty, S.P. Kinetic study of synthesis of bio-fuel additives from glycerol using a heteropolyacid. *Resour. Technol.* **2017**, *3*, 337–341. [CrossRef]

56. Xu, C.; Gan, J.; Mei, X.; Zhou, Y.; Duanmu, J.; Zhu, G.; Zhang, H.; Han, X.; Wang, Y.; Liu, S.-B. Highly Active silver ion-exchanged silicotungstic acid catalysts for selective esterification of glycerol with lauric acid. *Catal. Lett.* **2020**, *150*, 3584–3597. [CrossRef]

57. Chaves, D.M.; Ferreira, S.O.; Chagas da Silva, R.; Natalino, R.; José da Silva, M. Glycerol esterification over Sn(II)-exchanged Keggin heteropoly salt catalysts: Effect of thermal treatment temperature. *Energy Fuels* **2019**, *33*, 7705–7716. [CrossRef]

58. Melero, J.A.; Vicente, G.; Morales, G.; Paniagua, M.; Moreno, J.M.; Roldán, R.; Ezquerro, A.; Pérez, C. Acid-catalyzed etherification of bio-glycerol and isobutylene over sulfonic mesostructured silicas. *Appl. Catal. A* **2008**, *346*, 44–51. [CrossRef]

59. Celdeira, P.A.; Gonçalves, M.; Figueiredo, F.C.A.; Bosco, S.M.D.; Mandelli, D.; Carvalho, W.A. Sulfonated niobia and pillared clay as catalysts in etherification reaction of glycerol. *Appl. Catal. A* **2014**, *478*, 98–106. [CrossRef]

60. Pinto, B.P.; de Lyra, J.T.; Nascimento, J.A.C.; Mota, C.J.A. Ethers of glycerol and ethanol as bioadditives for biodiesel. *Fuel* **2016**, *168*, 76–80. [CrossRef]

61. Frusteri, F.; Cannilla, C.; Bonura, G.; Spadaro, L.; Mezzapica, A.; Beatrice, C.; di Blasio, G.; Guido, C. Glycerol ethers production and engine performance with diesel/ethers blend. *Top. Catal.* **2013**, *56*, 378–383. [CrossRef]

62. Marchionna, M.; Patrini, R.; Sanfilippo, D.; Paggini, A.; Giavazzi, L.P. From natural gas to oxygenates for cleaner diesel fuels. In *Studies in Surface Science and Catalysis*; Elsevier: Amsterdam, The Netherlands, 2001; Volume 136, pp. 489–494.

63. Srinivas, M.; Raveendra, G.; Parameswaram, G.; Prasad, P.S.S.; Lingaiah, N. Cesium exchanged tungstophosphoric acid Supported on tin oxide: An efficient solid acid catalyst for etherification of glycerol with *tert*-butanol to synthesize biofuel additives. *J. Mol. Catal. A* **2016**, *413*, 7–14. [CrossRef]

64. Da Silva, M.J.; Julio, A.A.; Ferreira, S.O.; da Silva, R.C.; Chaves, D.M. Tin(II) Phosphotungstate Heteropoly Salt: An Efficient solid catalyst to synthesize bioadditives ethers from glycerol. *Fuel* **2019**, *254*, 115607–115618. [CrossRef]

65. Da Silva, M.J.; Chaves, D.M.; Ferreira, S.O.; da Silva, R.C.; Filho, J.B.G.; Bruziquesi, C.G.O.; Al-Rabiah, A.A. Impacts of Sn(II) doping on the Keggin heteropolyacid-catalyzed etherification of glycerol with tert-butyl alcohol. *Chem. Eng. Sci.* **2022**, *247*, 116913–116929. [CrossRef]

66. Serafim, H.; Fonseca, I.M.; Ramos, A.M.; Vital, J.; Castanheiro, J.E. Valorization of glycerol into fuel additives over zeolites as catalysts. *Chem. Eng. J.* **2011**, *178*, 291–296. [CrossRef]

67. Alptekin, E.; Canakci, M. Performance and emission characteristics of solketal-gasoline fuel blend in a vehicle with spark ignition engine. *Appl. Therm. Eng.* **2017**, *124*, 504–509. [CrossRef]

68. Mota, C.J.A.; da Silva, C.X.A.; Rosenbach, N.; Costa, J.; da Silva, F. Glycerin Derivatives as Fuel Additives: The Addition of Glycerol/Acetone Ketal (Solketal) in gasolines. *Energy Fuels* **2010**, *24*, 2733–2736. [CrossRef]

69. Zahid, I.; Ayoub, M.; Abdullah, B.B.; Nazir, M.H.; Ameen, M.; Zulqarnain; Yusoff, M.H.M.; Inayat, A.; Danish, M. Production of fuel additive solketal via catalytic conversion of biodiesel-derived glycerol. *Ind. Eng. Chem. Res.* **2020**, *59*, 20961–20978. [CrossRef]

70. Charson, N.; Amnuaypanich, S.; Soontaranon, S.; Rugmai, S.; Amnuaypanich, S. Increasing solketal production from the solventless ketalization of glycerol catalyzed by nanodispersed phosphotungstic acid in poly(N-methyl-4-vinylpyridinium) grafted on silica nanoparticles. *J. Ind. Eng. Chem.* **2022**, *112*, 233–243. [CrossRef]

71. Sandesh, S.; Halgeri, A.B.; Shanbhag, G.V. Utilization of renewable resources: Condensation of glycerol with acetone at room temperature catalyzed by organic–inorganic hybrid catalyst. *J. Mol. Catal. A* **2015**, *401*, 73–80. [CrossRef]

72. Da Silva, M.J.; Teixeira, M.G.; Chaves, D.M.; Siqueira, L. An efficient process to synthesize solketal from glycerol over tin(II) silicotungstate catalyst. *Fuel* **2020**, *281*, 118724. [CrossRef]

73. Da Silva, M.J.; Rodrigues, A.A.; Teixeira, M.G. Iron (III) silicotungstate: An efficient and recyclable catalyst for converting glycerol to solketal. *Energy Fuels* **2020**, *34*, 9664–9673. [CrossRef]

74. Chaves, D.M.; da Silva, M.J. A selective synthesis of glycerol carbonate from glycerol and urea over Sn(OH)$_2$: A solid and recyclable in situ generated catalyst. *New J. Chem.* **2019**, *43*, 3698–3706. [CrossRef]

75. Srikanth, A.; Viswanadham, B.; Kumar, V.P.; Anipindi, N.R.; Chary, K.V.R. Synthesis and characterization of Cs-exchanged heteropolyacid catalysts functionalized with Sn for carbonolysis of glycerol to glycerol carbonate. *Appl. Petrochem. Res.* **2016**, *6*, 145–153. [CrossRef]

76. Narkhede, N.; Patel, A. Sustainable valorisation of glycerol via acetalization as Well as carboxylation reactions over silicotungstates anchored to zeolite Hβ. *Appl. Catal. A* **2016**, *515*, 154–163. [CrossRef]